JOURNAL OF THE Electrochemical Society

LIBRARY
UNIVERSITY OF UTAH
SALT LAKE CITY

Vol. 98, No. 9 September, 1951

Published Monthly by

THE ELECTROCHEMICAL SOCIETY

Uniformity

GLC Anodes for the electrolytic industry are uniform—they stand the test of comparison.

Baking Furnaces
Morganton,
N. C. Plant

Plants:
Niagara Falls, N. Y.
Morganton, N. C.

Great Lakes Carbon Corporation

GLC

ELECTRODE DIVISION · NIAGARA FALLS, N. Y.

Sales Offices:
Niagara Falls, N. Y.
New York, N. Y.
Chicago, Ill.
Pittsburgh, Pa.
Birmingham, Ala.
Wilmington, Cal.

PRODUCTS OF GREAT LAKES CARBON CORPORATION

Electrode Division
Graphite anodes. Graphite and amorphous carbon electrodes. Carbon and graphite specialties.

Oil and Gas Division
Crude petroleum and natural gas.

Carbon Division
Petroleum coke. Calcined petroleum coke. Industrial carbons.

Dicalite Division
Diatomaceous silica for filter-aids, fillers and insulating uses.

Perlite Division
Perlite lightweight aggregates and products for the building, oil, foundry and other industries. Perlite ore.

Merchant Coke Plant
Premium foundry and industrial coke. Coke co-products.

Journal of the

Electrochemical Society

SEPTEMBER, 1951 VOLUME 98 • NUMBER 9

CONTENTS

The Role of the Cation in the Electrical Double Layer. *David C. Grahame* 343

The Difference Effect on Titanium Dissolving in Hydrofluoric Acid. *M. E. Straumanis and P. C. Chen* 351

The Zirconia-Yttria System. *Pol Duwez, Frank H. Brown, Jr., and Francis Odell* 356

Luminescence of Three Forms of Zinc Orthophosphate:Mn. *Arthur L. Smith* 363

Cathodoluminescence Characteristics of Some Barium-Zinc-Silicate Phosphors with Manganese Activator. *Simon Larach* 369

The Thermoluminescence Characteristics of Silicate Phosphors Activated by Manganese and Arsenic. *C. Bull and G. F. J. Garlick* 371

The Effect of Temperature on Emission of Fluorescent Lamp Phosphors. *Charles W. Jerome* 376

Current Affairs

Plant Visits for Detroit Meeting to Include Dow, Ford, Chrysler 123C

News Notes 125C

Meetings of Other Organizations 125C

Activities of the Board of Directors 126C

Personals 126C

New Members 127C

Recent Patents 127C

Notes from Industry 128C

Employment Situations 128C

EDITORIAL STAFF

R. M. BURNS, *Chairman*

NORMAN HACKERMAN, *Technical Editor* ELEANOR REID, *Managing Editor* F. L. LAQUE, *Business Manager*
CECIL V. KING, *Associate Editor* MARY F. MURRAY, *Assistant Editor* U. B. THOMAS, *News Editor*

DIVISIONAL EDITORS: J. M. BIALOSKY, *Corrosion*; ABNER BRENNER, *Electrodeposition*; N. C. CAHOON, *Battery*; H. C FROELICH, *Electronics*; W. C. GARDINER, *Industrial Electrolytic*; S. J. SINDEBAND, *Electrothermic*; R. R. RALSTON, *Electric Insulation*; L. B. ROGERS, *Theoretical*; SHERLOCK SWANN, JR., *Electro-Organic*

REGIONAL EDITORS: JOSEPH A. SCHULEIN, *Pacific Northwest*; J. C. SCHUMACHER, *Los Angeles*; O. W. STOREY, *Chicago*; G. W. HEISE, *Cleveland*; PAUL S. BRALLIER, *Niagara Falls*; OLIVER OSBORN, *Houston*; EARL A. GULBRANSEN, *Pittsburgh*; J. W. CUTHBERTSON, *Great Britain*; T. L. RAMA CHAR, *India*

ADVERTISING: Richard Rimbach Associates—James Condon, 36 Myrtle St., *Boston;* Richard Rimbach, Jr., 551 Fifth Ave., *New York;* William J. Gallagher, 3701 N. Broad St., *Philadelphia;* C. F. Goldcamp, 921 Ridge Ave., *Pittsburgh;* Harold Haskett, 360 N. Mich. Ave., *Chicago;* James R. Wright, 411 N. Tenth St., *St. Louis;* M. D. Pugh, 2721 N. Marengo Ave., *Altadena* (*Los Angeles*).

Published monthly by The Electrochemical Society, Inc., Mt. Royal and Guilford Aves., Baltimore 2, Md., combining the JOURNAL and TRANSACTIONS OF THE ELECTROCHEMICAL SOCIETY. Editorial Office: 235 W. 102nd St., New York 25, N. Y. Business Office: Mt. Royal and Guilford Aves., Baltimore 2, Md., or 235 W. 102nd St., New York 25, N. Y. Statements and opinions given in articles and papers in the JOURNAL OF THE ELECTROCHEMICAL SOCIETY are those of the contributors, and The Electrochemical Society assumes no responsibility for them. Subscription: $8.50 to members, $12.00 to nonmembers. Single copies $1.00 to members, $1.25 to nonmembers. Copyright 1951 by The Electrochemical Society. Entered as second-class matter November 15, 1947, at the Post Office at Baltimore, Md under the act of August 24, 1912.

Electrochemistry at Dow

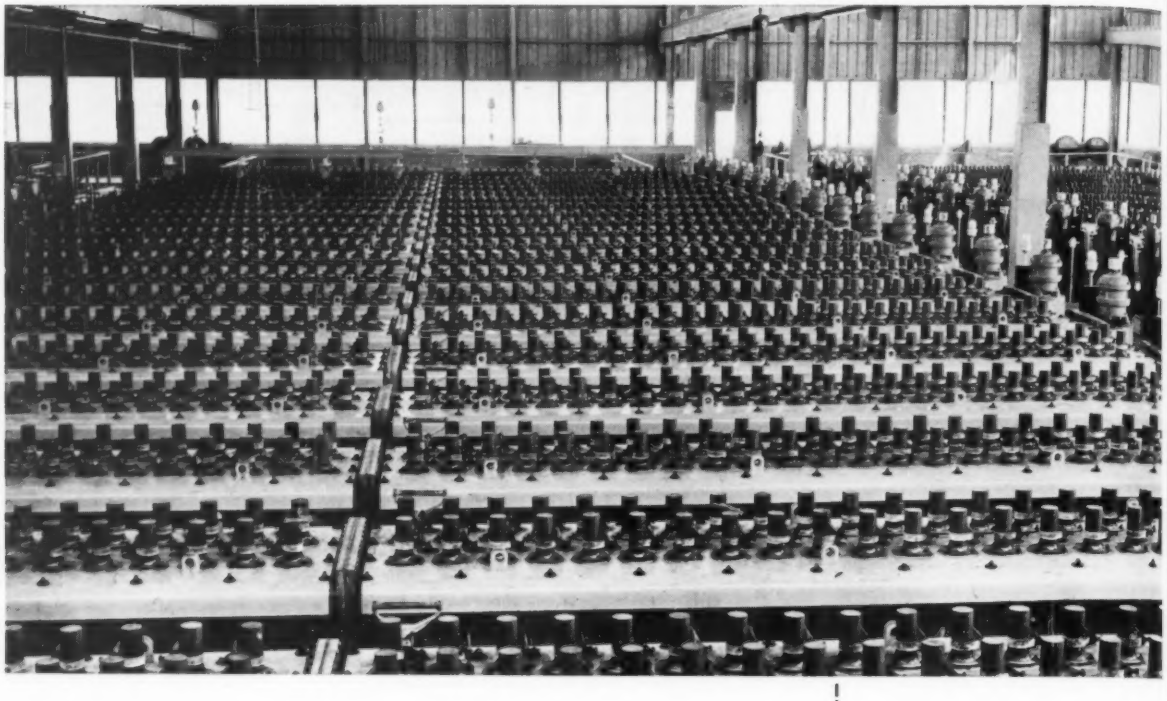

Today's Efficiency from Yesterday's Research

Every day in electrochemistry sees the advent of a new idea, a new process to improve the older methods. From this progressing research, more efficient methods are developed to serve all industry with higher grade, more abundant materials.

A typical example of electrochemistry's research is the development of the horizontal type mercury cell. This new revolutionary cell efficiently produces high purity caustic soda and chlorine for the most exacting demands of industry. It seems to be a fitting successor to the well-known Castner "Rocking cell" (shown at right)—which was so well conceived by H. Y. Castner in early 1900 that his basic design is still used, with only slight modification and improvement.

However, as many cases prove, electrochemical research never ceases . . . and, undoubtedly, new improvements will be made in the future on the horizontal type mercury cell. Dow has been glad to participate in this dynamic surge in electrochemistry. In the future, as in the past, Dow will continue to devote its energies and resources toward better methods, better products . . . through electrochemistry.

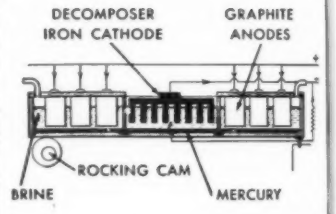

CASTNER "ROCKING CELL"

THE DOW CHEMICAL COMPANY
MIDLAND, MICHIGAN

DOW

CHEMICALS

INDISPENSABLE TO INDUSTRY AND AGRICULTURE

Editorial

Solid State Electrochemistry

ELECTROCHEMISTS have expressed concern about the scant attention given electrochemistry in present-day college curricula. There can be no doubt that men are not being trained for the electroprocess industries and that these industries, comprising as they do one of the largest segments of American chemical industry, are forced to develop their own industrial electrochemists out of chemists, chemical engineers, and metallurgists—admittedly good raw material with which to start. Part of the pessimism concerning the lack of electrochemical training may arise from a restricted view of what comprises electrochemistry. The notable accomplishments of classical electrochemistry were mainly in the liquid state and to a lesser extent in gases. Only recently has the solid state received attention. Professor Carl Wagner, who is to be the Society's first Palladium Medalist, was among the first to make significant contributions to this field. It is of interest to note that leadership in solid state research has been assumed by industry and with fruitful results. Among important developments has been a major contribution to electronics in what is known as the transistor. In its present state of development, this consists essentially of a small piece of germanium in which the flow of electrons and "holes" is subject to external control. Thus it becomes possible to perform many of the functions of a vacuum tube and some things not heretofore possible in ordinary electronics. These and other related developments have given rise to new concepts and a new technology. They appear to have large industrial potentialities. Dean Ridenour commenting in the *Scientific American* upon the revolutionary contribution and brilliant future of the transistor says: ". . . there is nothing wrong with electronics that elimination of vacuum tubes would not fix!"

If the older art of the electroprocess industries has been neglected in the universities, it has been succeeded in their crowded curricula by instruction in the newer theories and tools of physics and chemistry upon which future progress in electrochemistry must depend. The first paper presented before The Electrochemical Society was "A University Course in Electrochemistry." Fifty years later in 1952 the same title will be appropriate, but how changed the subject matter! —RMB

FUTURE MEETINGS OF
The Electrochemical Society

Detroit, October 9, 10, 11, and 12, 1951

Sessions on

Corrosion, Electrodeposition, Electro-Organic Chemistry

Round Tables on Power Supply and Requirements for Electrochemical Industries, Batteries, and Screen Engineering

Headquarters at the Statler Hotel

* * *

Philadelphia, May 4, 5, 6, 7, and 8, 1952

FIFTIETH ANNIVERSARY MEETING

Sessions on

Electric Insulation, Electrothermics, Instrumentation, Luminescence, Methods of Applying Phosphors, Rare Metals, Theoretical Electrochemistry

Headquarters at the Benjamin Franklin Hotel

* * *

Montreal, October 27, 28, 29, 30, and 31, 1952

Headquarters at the Mt. Royal Hotel

* * *

New York, April 12, 13, 14, 15, and 16, 1953

Headquarters at the Statler Hotel

Papers are now being accepted for the meeting to be held in Philadelphia. Abstracts (not exceeding 75 words in length) are due at the Secretary's Office, 235 West 102nd Street, New York 25, N. Y., *not later than February 1, 1952.* Complete manuscripts should be sent in triplicate to the Editor of the JOURNAL at the same address.

The Role of the Cation in the Electrical Double Layer[1,2]

DAVID C. GRAHAME

Moore Laboratory of Chemistry, Amherst College, Amherst, Massachusetts

ABSTRACT

The differential capacity of a number of tenth-normal aqueous solutions of metallic chlorides has been measured as a function of potential. The results are interpreted to mean that the solvent sheaths on the positive and negative ions are displaced as the ions approach the interface. New explanations are given for several well-known phenomena connected with the double layer. The surface charge density and integral capacity of the non-diffuse part of the electrical double layer have been calculated from these data. The ratios of the differential capacities have been found to approach unity at potentials where the concentration of cations within the double layer is at a minimum.

The experimental study of the electrical double layer has been made much more exact in recent years through the investigation of the differential capacity of metal-solution interfaces using alternating current bridge techniques (1–5). The differential capacity is thermodynamically related to the interfacial tension, the surface charge density, and to the concentrations of the individual ions making up the double layer. These matters are discussed in a recent review paper (6).

The present work has to do with a comparison of the differential capacities of mercury in tenth-normal aqueous solutions of various metallic chlorides at 25°C. The differences are comparatively small, so small that it was not known at the beginning of this work whether or not it would be possible to measure them at all. The only comparable work is that of Gouy (7) who measured the *interfacial tension* of a large number of electrolytic solutions and found that the differences attributable to the choice of cation were so small that one could not clearly distinguish them from the effects of experimental error. Nevertheless it is interesting to note that those differences specifically mentioned by Gouy as being probably real reappear in the present work as the largest of the effects observed.

EXPERIMENTAL PROCEDURE

The method by which differential capacity measurements are made in this Laboratory has been described elsewhere (3). The only change involved in the present work was the addition of a second solution reservoir so arranged that two deaerated solutions could be introduced alternately into the working cell with intermediate rinsing. One of the two solutions was generally tenth-normal potassium chloride, whose differential capacity values were accurately known from previous work (3); the other was a solution of the electrolyte to be tested. The ratio of the capacities of the two solutions at any one potential could be determined without much difficulty to within about 1 per cent, or better if the occasion seemed to warrant. The data presented in this paper are believed to be accurate to within about ½ per cent except at the extremes of potential, where the error rises somewhat.

It is possible to carry out the measurements here reported without the introduction of liquid junctions. This could be done by measuring all potentials relative to an electrode reversible to the common anion in the solution under test. In practice this result was achieved by making two identical but opposed liquid junctions, the only assumption being that the two junctions really were identical in potential. Owing to the relatively small effect of potential upon capacity in the major part of the potential range investigated, this assumption was amply justified.

The solutions were deaerated with tank nitrogen, which was not generally treated further since experience had shown such treatment to be without effect. The solutions were made up in conductivity water ($\rho < 1.1 \times 10^{-6}$ ohm^{-1}/cm) from purified materials. Hydrochloric acid was freshly distilled in an all-Pyrex apparatus; the salts were purified by recrystallization in fused silica dishes. (Using these vessels, it was found possible to recrystallize even aluminum chloride and zinc chloride from hydrochloric acid.) The number of recrystallizations employed depended somewhat upon the yield per crystallization, but was generally two. Comparison of purified and unpurified (C.P.) materials revealed small differences, especially at potentials more anodic than that of the electrocapillary maximum (e-c max). In addition a

[1] Manuscript received January 9, 1951. This paper prepared for delivery before the Washington Meeting, April 8 to 12, 1951.

[2] This paper is a condensation of a report to the Office of Naval Research dated March 9, 1950, and available at the Library of Congress. Requests for copies may also be directed to the author.

rather marked effect on the series *resistance* was noted at a potential of about 0.25 volt. A minor maximum of resistance was observed there in unpurified materials, and its absence served as a practical criterion of purity. We attribute the effect to the presence of traces of iron in the C.P. salts, but were unable to duplicate the effect by adding ferric ion to purified materials. The matter was not investigated extensively, however.

A frequency of 1000 cycles was used throughout. The results do not depend upon this choice to any significant extent (2).

If q is the charge and E the potential of a condenser, what is measured by an impedance bridge when the input voltage is small is not q/E, the integral capacity, but dq/dE, the differential capacity. If the capacity is independent of the potential, $q/E = dq/dE$, but not otherwise. In studies of the electrical double layer, the capacity is not independent of the potential.

TABLE I.* *Differential capacity of mercury in tenth-normal solutions of metallic chlorides at 25°C. Potentials measured relative to calomel electrode in same solution*

E volts	Capacity in microfarads per square centimeter							
	LiCl	NaCl	KCl	RbCl	CsCl	HCl	NH_4Cl	$MgCl_2$
0.063	94.1	94.9	97.2	102.4	103.8	95.4	96.6	94.1
0.08	72.0	72.7	73.8	76.5	77.4	72.6	73.4	74.7
0.12	52.1	52.4	52.8	54.0	54.2	52.2	52.6	54.2
0.16	44.52	44.61	44.79	45.51	45.51	44.39	44.66	45.64
0.24	38.67	38.58	38.64	39.04	38.95	38.37	38.54	39.14
0.32	38.43	38.35	38.37	38.53	38.51	38.15	38.45	38.62
0.41	39.84	39.85	39.85	39.84	39.96	39.76	39.87	39.93
0.46	38.62	38.58	38.67	38.63	38.75	38.73	38.66	38.77
0.54	31.75	31.82	31.88	31.88	32.08	32.21	31.90	32.37
0.62	24.58	24.72	24.78	24.85	25.32	25.03	24.85	26.03
0.70	21.00	21.19	21.31	21.44	22.12	21.10	21.43	22.68
0.86	17.90	18.14	18.30	18.57	19.27	17.62	18.50	18.59
1.00	16.32	16.57	16.77	17.11	17.86	16.12	17.07	16.71
1.16	15.46	15.78	16.06	16.50	17.29		16.45	15.78
1.32	15.47	15.87	16.28	16.86	17.66		16.88	15.96
1.48	16.17	16.64	17.22	17.93	18.67		18.16	16.89
1.64	17.42	17.80	18.70	19.51	20.21			18.51
1.80	19.00	19.24	20.76	21.66	22.32			20.52
1.94	21.37	21.76	24.03	25.02	25.76			

E volts	Capacity in microfarads per square centimeter								
	$CaCl_2$	$SrCl_2$	$BaCl_2$	$MnCl_2$	$CoCl_2$	$NiCl_2$	$AlCl_3$	$LaCl_3$	$PrCl_3$
0.063	99.2	96.4	103.6	99.1	98.7	99.7	98.5	106.0	107.4
0.08	75.9	77.5	78.7	75.6	75.4	76.0	77.0	80.0	80.7
0.12	54.3	54.9	55.3	54.0	54.0	54.2	55.0	56.3	56.6
0.16	45.82	46.09	46.36	45.60	45.64	45.78	46.18	46.98	47.25
0.24	39.16	39.27	39.34	38.98	39.10	39.18	39.41	39.71	39.73
0.32	38.65	38.71	38.73	38.67	38.63	38.78	38.98	39.15	38.65
0.41	39.82	40.09	40.16	40.03	40.03	40.17	40.34	40.49	39.56
0.46	38.51	38.92	38.98	38.79	38.74	39.02	38.94	39.22	38.31
0.54	32.10	32.50	32.59	32.29	32.31	32.39	32.37	32.82	32.18
0.62	26.12	26.49	26.53	26.06	26.14	26.27	26.83	27.30	26.79
0.70	22.85	23.06	23.11	22.70	22.72	22.81	23.63	23.88	23.42
0.86	18.81	18.89	18.89	18.67	18.71	18.71	19.02	19.26	18.98
1.00	16.92	16.98	16.97	16.79	16.74		16.90	17.29	17.09
1.16	16.12	16.25	16.25	16.02				16.51	16.39
1.32	16.40	16.59	16.62	16.33				16.94	16.86
1.48	17.49	17.63	17.64						
1.64	19.13	19.11	19.11						
1.80	20.91	20.63	20.96						

* A much larger table of values is presented in Reference 10. Also, for extended version of tables, order Document 3292 from the American Documentation Institute, 1719 N Street, N. W., Washington 6, D. C., remitting $1.00 for microfilm or $1.35 for photocopies (6 x 8 in.).

Results and Discussion

Table I summarizes the results of the measurements. The uncertainty in the *absolute values* is estimated to be about $C^2/1000$ per cent, where C is expressed in $\mu f/cm^2$. The *relative* values of consecutive entries are uncertain by two or three units in the last place. The ratio of two entries for different substances at a given potential is uncertain by about 0.5 per cent except at very low potentials where it increases to 1 or 2 per cent.

The most conspicuous fact to be observed in Table I is that the character of the cation makes only very small differences in the differential capacity of the electrical double layer. It needs to be realized in this connection that the differential capacity is a very sensitive function and tends to magnify such differences as do exist. The largest differences observed are among the univalent cations (in agreement with the results of Gouy), cesium giving in general the highest capacities and lithium giving the lowest. When the potential is greater than about 0.7 volt, anions are almost completely expelled from the double layer by coulombic repulsion, so that it is above this potential that the effects of the cation are revealed in their most characteristic form.

Integration of the capacity with respect to potential gives the surface charge density of electrons, q, as has been discussed in previous publications (3). The constant of integration is obtained from the potential of the electrocapillary maximum by noting (from the Lippmann equation) that the surface charge density is zero at that potential. Measurements of the potential of the e-c max have been made for this purpose and reported elsewhere[3] (8). The results are presented at the bottom of Table II.

The integration of the capacity has been carried out by numerical means using a method previously described (3). The results are presented in Table II and are used in the computation of Table III.

In the interpretation of the results it is convenient to divide the solution phase of the double layer into two parts, the diffuse and non-diffuse parts, separated by the outer Helmholtz plane. The diffuse part is that part populated by an ionic atmosphere of the type described by Gouy (11). The outer Helmholtz plane is the plane of closest approach to the mercury surface of the centers of the cations. The non-diffuse part of the double layer lies between the mercury surface and the outer Helmholtz plane. It will be assumed as usual that anions can come into contact with the mercury surface, their solvent sheaths being pushed aside. Whether or not cations can do the same will be discussed below. (It is concluded that they can.)

The potential of the outer Helmholtz plane can be calculated by the kinetic theory of the diffuse double layer (6). The potential drop across the non-diffuse double layer can then be obtained by difference from the total potential drop[4]. The ratio of the surface charge density, q, to the potential drop across the non-diffuse part of the double layer will be called K^{nd} and is probably the most significant quantity that can be calculated from the results presented in this paper. It is an *integral* capacity, which makes it less sensitive to small influences than a differential capacity, and small differences are therefore to be regarded as significant. It represents the electrical condition of the region between the mercury surface and the outer Helmholtz plane in the most direct manner possible. Since the capacity of a parallel plate condenser is proportional to D/d (where D is the dielectric constant and d is the distance between the plates) K^{nd} may be regarded as a measure of the effective value of this ratio.

A comparison of K^{nd} values for different solutions should be made, not at common values of potential, but at common values of the surface charge density, q. This is desirable because it produces the same electrical charge on the faces of the hypothetical condenser of which the non-diffuse double layer is the dielectric.

Values of K^{nd} calculated in the manner described are presented in Table III. Since the calculation is only significant in the absence of anion adsorption, values are given only for potentials where the anions are almost completely expelled from the interface (see above). For convenience the *ratios* of K^{nd} values are shown in Table IV. One notices first that all the ratios are close to unity, signifying that the nature of the cation is of minor importance. This result is quite unexpected and signifies either that the cations remain hydrated in the interface (in which case they would be expected to act like hydrated point charges) or else that the electrical properties of the interface are determined primarily by the dielectric properties of the solvent. This point is discussed further below,

[3] This report is available at the Library of Congress. Requests for copies may also be directed to the author.

[4] An extensive discussion of this point is given in Reference 6. The assumption is there made that in the absence of anion adsorption the potential of the e-c max of the solutions investigated would be 0.480 volt, relative to a normal calomel electrode. [A more recent investigation (Reference 8, page 15) makes this value closer to 0.472 volt, which is the value used in the computation of Table III.] This assumption is suggested by a study of solutions whose anions are not adsorbed. Potentials calculated in this way have been termed *rational* potentials because they take into account those sources of potential which are known and ignore those which are not susceptible to measurement.

TABLE II.* *Surface charge density, q, of the electrical double layer in tenth-normal aqueous solutions of metallic chlorides at 25°C*

E volts	q in μcoul/cm²							
	LiCl	NaCl	KCl	RbCl	CsCl	HCl	NH_4Cl	$MgCl_2$
0.08	19.59	19.58	19.66	19.68	19.70	19.40	19.60	19.84
0.16	15.28	15.25	15.28	15.26	15.26	15.14	15.26	15.39
0.30	9.72	9.70	9.70	9.64	9.65	9.62	9.71	9.75
0.50	1.942	1.941	1.942	1.870	1.872	1.879	1.932	1.964
0.70	−3.44	−3.46	−3.48	−3.53	−3.61	−3.55	−3.48	−3.64
1.10	−10.49	−10.61	−10.70	−10.87	−11.44		−10.80	−10.98
1.50	−16.74	−17.01	−17.26	−17.66	−18.32		−17.60	−17.42
1.80	−22.00	−22.38	−22.93	−23.57	−24.45			−23.03
1.95	−25.04	−25.45	−26.28	−27.08	−28.06			
e-e max volts	0.5592	0.5591	0.5589	0.5576	0.5564	0.5566	0.5587	0.5590

E volts	q in μcoul/cm²								
	$CaCl_2$	$SrCl_2$	$BaCl_2$	$MnCl_2$	$NiCl_2$	$CoCl_2$	$AlCl_3$	$LaCl_3$	$PrCl_3$
0.08	19.86	19.99	20.06	19.80	19.89	19.81	20.03	20.23	20.14
0.16	15.37	15.46	15.48	15.37	15.44	15.37	15.50	15.61	15.43
0.30	9.71	9.79	9.80	9.75	9.79	9.74	9.81	9.87	9.68
0.50	1.940	1.968	1.969	1.948	1.958	1.943	1.948	1.979	1.945
0.70	−3.67	−3.70	−3.71	−3.65	−3.66	−3.66	−3.76	−3.79	−3.74
1.10	−11.10	−11.17	−11.18	−11.02		−11.03		−11.42	−11.28
1.40	−15.99	−16.10	−16.12	−15.89				−16.45	−16.28
1.80	−23.49	−23.60	−23.64						
e-e max volts	0.5586	0.5588	0.5587	0.5589	0.5588	0.5585	0.5585	0.5588	(0.5588)

* A much larger table of values is presented in Reference 10. A larger set is also included in the document mentioned in the footnote to Table I. The values appearing in Reference 10 differ very slightly from the others because they are referred to older and slightly less exact values of the potential of the e-e max. For any one substance, the difference in q is a constant.

TABLE III.* *Integral capacity, K^{nd}, of the non-diffuse part of the electrical double layer in tenth-normal aqueous solution at 25°C*

$-q$ μcoul/cm²	Microfarads per cm²							
	LiCl	NaCl	KCl	RbCl	CsCl	HCl	NH_4Cl	$MgCl_2$
6	25.03	25.28	25.34			25.58	25.67	23.78
8	23.50	23.80	23.89	24.30	25.26	23.67	24.19	22.62
10	22.07	22.40	22.55	22.98	23.97	22.17	22.87	21.44
12	20.96	21.30	21.51	21.95	22.93		21.86	20.45
14	20.15	20.50	20.74	21.23	22.18		21.14	19.72
16	19.62	19.99	20.27	20.77	21.70		20.71	19.25
18	19.32	19.69	20.01	20.52	21.40		20.51	19.01
20	19.21	19.55	19.92	20.44	21.27			18.94
22	19.21	19.54	19.96	20.49	21.27			19.00
24	19.32	19.63	20.10	20.63	21.37			19.16
26			20.36	20.82	21.55			

$-q$ μcoul/cm²	Microfarads per cm²								
	$CaCl_2$	$SrCl_2$	$BaCl_2$	$MnCl_2$	$CoCl_2$	$NiCl_2$	$AlCl_3$	$LaCl_3$	$PrCl_3$
4							24.90	25.56	25.05
6	24.51	24.93	25.01	24.63	24.67	24.85	24.37	24.93	24.42
8	23.28	23.53	23.60	23.28	23.28	23.47	23.08	23.63	23.15
10	21.94	22.22	22.26	21.94	21.94		21.80	22.36	21.91
12	20.91	21.16	21.19	20.87	20.84			21.29	20.91
14	20.17	20.41	20.42	20.13				20.54	20.21
16	19.71	19.93	19.95	19.66				20.06	
18	19.48	19.67	19.70						
20	19.41	19.59	19.60						
22	19.46	19.60	19.63						
24	19.59	19.79	19.74						

* Computed on the assumption that the potential of the normal calomel electrode has a rational potential of 0.472 volt. See footnote 4.

showing the second alternative to be much the more probable.

Although the ratios in Table IV are close to unity, a marked trend is nevertheless observable within a given group of elements and always in the same direction. Thus from lithium to cesium K^{nd} increases regularly, and the same is true of the alkaline earth metals. One might have expected the opposite trend, since a large ion such as cesium would not be expected to approach the interface as closely as a small ion such as lithium. A larger separation of charge

TABLE IV. *Ratios of the integral capacities of the non-diffuse part of the electrical double layer in tenth-normal aqueous solutions of metallic chlorides at 25°C*

$-q$ μcoul/cm²	LiCl / KCl	NaCl / KCl	RbCl / KCl	CsCl / KCl	HCl / KCl	NH_4Cl / KCl	$BaCl_2$ / KCl	$LaCl_3$ / KCl
6	0.988	0.998			1.009	1.013	0.987	0.984
8	0.984	0.996	1.017	1.057	0.991	1.013	0.988	0.989
10	0.979	0.993	1.019	1.063	0.983	1.014	0.987	0.992
12	0.974	0.990	1.020	1.066		1.016	0.985	0.990
14	0.972	0.988	1.024	1.069		1.019	0.985	0.990
16	0.968	0.986	1.025	1.071		1.022	0.984	0.990
18	0.966	0.984	1.025	1.070		1.025	0.985	
20	0.964	0.981	1.026	1.068			0.984	
22	0.964	0.979	1.027	1.066			0.984	
24	0.961	0.977	1.026	1.063			0.982	
26			1.023	1.058				

$-q$ μcoul/cm²	$MgCl_2$ / $BaCl_2$	$CaCl_2$ / $BaCl_2$	$SrCl_2$ / $BaCl_2$	$MnCl_2$ / $BaCl_2$	$CoCl_2$ / $BaCl_2$	$NiCl_2$ / $BaCl_2$	$AlCl_3$ / $LaCl_3$	$PrCl_3$ / $LaCl_3$
4							0.974	0.980
6	0.951	0.980	0.997	0.985	0.986	0.994	0.978	0.980
8	0.959	0.986	0.997	0.986	0.986	0.995	0.977	0.980
10	0.963	0.986	0.998	0.986	0.986		0.975	0.980
12	0.965	0.987	0.999	0.985	0.984			0.982
14	0.966	0.988	0.999	0.986				0.984
16	0.965	0.988	0.999	0.986				
18	0.965	0.989	0.999					
20	0.966	0.990	1.000					
22	0.968	0.991	0.999					
24	0.971	0.992	1.003					

would then produce a smaller capacity. A possible explanation which does fit the facts is suggested below.

The constancy of the ratios K^{nd} for a given pair of substances indicates in another way that the capacity is more strongly influenced by the dielectric properties of the solvent than of the solute.

Ion Solvation in the Double Layer

It is a matter of the first importance to the theory of the double layer to ascertain if possible whether or not the solvent sheath of the ions remains intact as the ions approach the interface. It is quite certain that the solvent sheath around most *anions* is pushed aside as the anions approach the surface. This is clearly shown by the fact that anions are in general readily adsorbed on a mercury surface, especially when it is positively charged. The adsorption may be shown to be largely chemisorption, meaning that covalent bonds are involved. But covalent bonds involve short range forces, and certainly could not act through a sheath of the solvent.

The situation is less clear with respect to cations. Since cations do not show specific adsorption in general, there is no opportunity to apply the argument used for anions. The arguments for and against cation hydration (on the side facing the metal) at the interface are presented below. It will be observed that the arguments against cation hydration effectively dispose of those *for* it.

Arguments For and Against the Assumption of Cation Hydration at the Interface of the Electrical Double Layer

For: In a moderately concentrated solution of an adsorbed electrolyte (adsorption being caused by covalent bonding of the anions to the metallic surface) the potential observed between the phases at the e-c max is greater than can be accounted for by the diffuse double layer theory. For example, in a 1.0*M* solution of potassium iodide the potential generated amounts to about 340 mv (6), whereas the potential of the outer Helmholtz plane is calculated to be about 65 mv and certainly not much more. This shows that there is a large potential gradient within the non-diffuse part of the double layer even at the potential of the e-c max. This must certainly arise from the inability of the cations to move in close enough to the interface to neutralize the charge of the anions. Since anions are normally larger than cations (in their unhydrated state), the conclusion which might be drawn is that the cations remain hydrated, making them effectively *larger* than the anions.

Against: A possible interpretation of the results described above is afforded by assuming that the adsorbed anions are strongly polarized. The centroid of negative charge of the adsorbed anions may be displaced toward the mercury surface, making it impossible for the cations to annul their electrical effects by moving into the plane of negative charge. This would be sufficient to produce the observed potential difference.

For: The capacity of the double layer when the mercury is negatively charged is almost independent of the nature of the cation. Since the cations have very different crystal radii, this effect is not to be expected unless the cations are hydrated and remain so at the interface. A series of hydrated cations of a given charge is surrounded by identical fields at distances greater than their crystal radii, and should therefore exhibit identical properties so long as the solvent sheath remains intact. Slight differences will arise to the extent that the medium does not behave like a continuous medium. However, it is not necessary to assume the absence of dielectric saturation effects, since these should be identical in the several cases.

Against: The facts are equally well explained by assuming that the nature of the solvent rather than

the specific properties of the attracted cations is the determining factor in the capacity measurements. The fact that polyvalent ions give the same capacity as univalent ions receives a much more natural explanation on this hypothesis. The slightly larger capacity exhibited by larger ions could be attributed to the smaller field strength at their surfaces, which would tend to diminish the effects of dielectric saturation in the non-diffuse part of the double layer. (It has been shown elsewhere (9) that dielectric saturation is not an important factor in determining the properties of the *diffuse* part of the double layer.)

For: The polyvalent cations are very much like one another and like the univalent ions in their electrocapillary properties. Therefore one must assume either that all are hydrated at the interface or else that all are unhydrated. But the energies of hydration of polyvalent ions are so great that it seems improbable that these lose their sheaths easily.

Against: The assumption that no energy is available to displace the hydration sheath is found on closer examination to be untenable. The free energy of hydration depends upon the magnitude of the factor $1 - 1/D$, where D is the dielectric constant, and is therefore approximately the same for any large value of D. But the dielectric constant of a metallic conductor is effectively infinite (Reference 10, footnote 9). Therefore the energy of solvation of an ion in contact with mercury is of the same order of magnitude as, and possibly a little larger than, the energy of solvation of an ion with water. Therefore the ion can exchange mercury for water in its solvent sheath without gain of free energy. The same conclusion is reached by a consideration of image forces. A cation approaching a mercury surface is attracted to its image. The energy required to remove the solvent sheath on one side of the ion is supplied by the approach of the ion to its oppositely charged image. This same argument explains why anions can approach the mercury surface without interference from the solvent sheath.

Against: If one could devise an electrostatic argument to support the contention that cations remain hydrated at the interface, then this same argument would presumably lead to the conclusion that anions also remain hydrated. But this is surely contrary to the facts.

Against: The electroreduction of cations is in many instances a reversible process. It is difficult to visualize an electron transfer without activation energy if the transfer takes place through a hydration sheath.

The arguments against cation hydration in the direction of the interface appear to be conclusive. The inner and outer Helmholtz planes should probably now be redefined as the planes of closest approach of the *electrical* centers of anions and cations, respectively. The electrical centers of cations are presumably not far removed from those of their geometrical centers, whereas those of the anions are displaced toward the metallic surface whenever chemisorption is involved. Thus the inner Helmholtz plane lies closer to the interface than the outer, as originally conceived (Reference 6, p. 466). The falling off of K^{nd} with increasing values of $-q$ (Table III) is readily explained as an effect of dielectric saturation in the *non-diffuse* part of the double layer. The very small final rise is probably to be attributed to deformation of the coulombically held cations. It is certainly not a manifestation of the reversible reduction of the cations (the so-called pseudo-capacity) as has sometimes been suggested. Pseudo-capacity appears at the reduction potential of the cation involved, whereas the effect here under discussion appears always at the same potential regardless of the nature of the cation.

It might appear that if a cation adsorbed on a mercury surface loses its hydration sheath, it is, to all intents, a metal *atom*, the needed electron or electrons being already present on the mercury surface. It is necessary to remember, however, that the electron transfer process is exoenergetic (ΔF positive) at potentials below the polarographic half-wave potential for the ion in question. This shifts the equilibrium strongly in favor of the unreduced state of the ion.

The data of Frumkin (12) and of Bowden and Grew (13) indicate that there is no direct relation between the dielectric constant of the solvent and the capacity of the double layer in the region of cathodic polarization. This result is not to be regarded as surprising or contradictory to the present discussion in view of the fact that the capacity of the non-diffuse part of the double layer (which is the controlling factor) is strongly influenced by dielectric saturation effects, and these bear little or no relation to the ordinary dielectric constant.

Positively Charged Surfaces

The considerations presented up to this point have been concerned with the properties of the electrical double layer at a negatively charged mercury surface. For a discussion of the uncharged or positively charged surface it is necessary to return to the differential capacities. For this purpose it is desirable to consider the *ratios* of the differential capacities instead of their absolute values. Fig. 1 to 6 show these ratios in graphical form. In addition to the characteristics discussed above it will be noted that the ratios approach unity at a potential of about 0.4 volt. This is the potential at which the concentration of the cations in the double layer also approaches a minimum in tenth-normal chloride solutions (at least for sodium and potassium chlorides and probably also in barium chloride, the only cases so far investigated). Since the electrical properties of the system are determined by the composition of the double layer, it is natural that an ion which is nearly absent should have little effect.

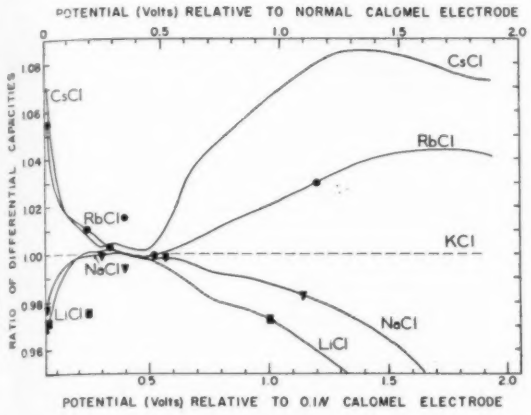

FIG. 1. Ratio of differential capacity of mercury-solution interface in tenth-normal aqueous solution of substance named to differential capacity in potassium chloride.

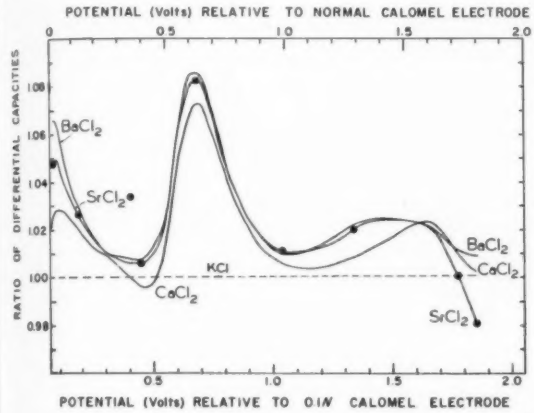

FIG. 2. Ratio of differential capacity of mercury-solution interface in tenth-normal aqueous solution of substance named to differential capacity in potassium chloride.

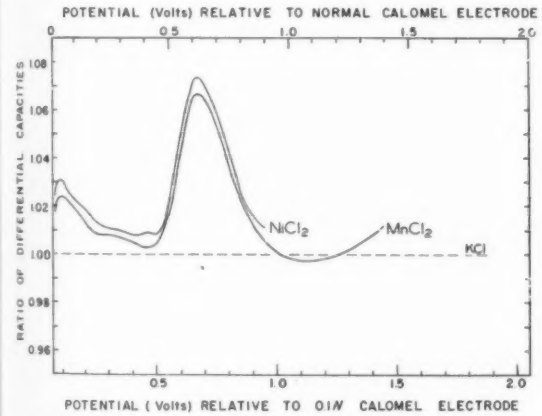

FIG. 3. Ratio of differential capacity of mercury-solution interface in tenth-normal aqueous solution of substance named to differential capacity in potassium chloride.

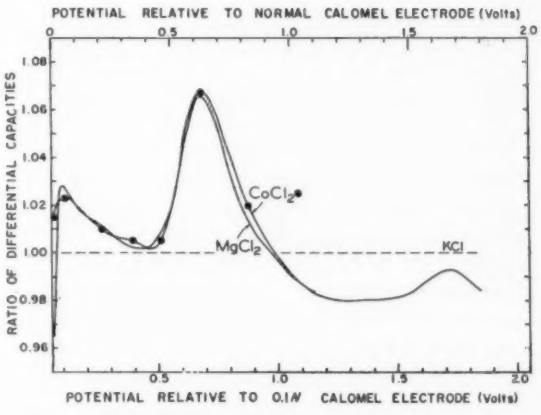

FIG. 4. Ratio of differential capacity of mercury-solution interface in tenth-normal aqueous solution of substance named to differential capacity in potassium chloride.

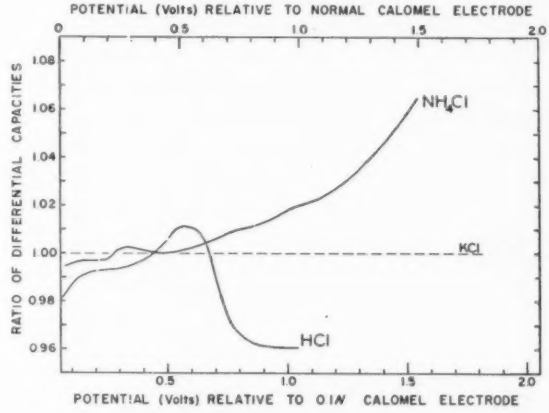

FIG. 5. Ratio of differential capacity of mercury-solution interface in tenth-normal aqueous solution of substance named to differential capacity in potassium chloride.

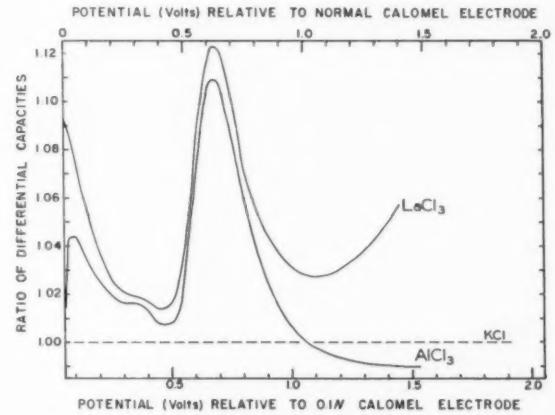

FIG. 6. Ratio of differential capacity of mercury-solution interface in tenth-normal aqueous solution of substance named to differential capacity in potassium chloride.

It might be supposed that the greater the positive charge on the mercury surface, the greater the repulsion of cations, but such is not the case. A positively charged surface forms covalent bonds with the anions in the solution, thereby holding anions of total charge greater than the positive charge on the mercury. As a result, the sum of the two layers of charge is negative, and cations are again attracted. This accounts for the fact that there is a potential at which the concentration of cations in the double layer is a minimum and also for the fact that cations again exert an effect upon the properties of the double layer when the mercury is more positively charged. The details of this latter effect are not yet understood, however.

The pronounced maxima in the ratios of the differential capacities shown in Fig. 2, 3, 4, and 6 for solutions containing divalent or trivalent cations are caused by the enhanced capacity of the *diffuse* double layer in the presence of these ions. This behavior is predicted by the theory of the diffuse double layer. It will be noted that K^{nd} does not exhibit this effect, which shows that it has been fully accounted for by the application of the theory to the experimental data. In the application of this theory to asymmetric electrolytes the usual equations, valid only for symmetrical electrolytes, were not employed. The extended equations, valid for any valence type and discussed in Reference 6, were used.

ACKNOWLEDGMENT

The support of the Research Corporation and of the Office of Naval Research is gratefully acknowledged.

Any discussion of this paper will appear in a Discussion Section, to be published in the June 1952 issue of the JOURNAL.

REFERENCES

1. D. C. GRAHAME, *J. Am. Chem. Soc.*, **63,** 1207 (1941).
2. D. C. GRAHAME, *Ibid.*, **68,** 301 (1946).
3. D. C. GRAHAME, *Ibid.*, **71,** 2975 (1949).
4. T. BORISOVA, B. ERSHLER, AND A. FRUMKIN, *J. Phys. Chem. (U.S.S.R.)*, **22,** 925 (1948); U. S. Naval Research Lab. Translation No. 306.
5. T. I. BORISOVA AND B. V. ERSHLER, *Ibid.*, **24,** 337 (1950); U. S. Naval Research Lab. Translation No. 307.
6. D. C. GRAHAME, *Chem. Revs.*, **41,** 441 (1947).
7. G. GOUY, *Ann. chim. et phys.* [7], **29,** 145 (1903).
8. D. C. GRAHAME, E. M. COFFIN, AND J. I. CUMMINGS, "Thermodynamic Properties of the Electrical Double Layer; Potential of the Electrocapillary Maximum in Aqueous Solution at 25°C," Technical Report No. 2 to the Office of Naval Research (Aug. 11, 1950).
9. D. C. GRAHAME, *J. Chem. Phys.*, **18,** 903 (1950).
10. D. C. GRAHAME, "Thermodynamic Properties of the Electrical Double Layer; Capacity of the Mercury-Solution Interface in Tenth-Normal Aqueous Solutions of Metallic Chlorides at 25°C and Derived Properties," Technical Report No. 1 to the Office of Naval Research (Mar. 9, 1950).
11. G. GOUY, *Compt. rend.*, **149,** 654 (1910).
12. A. FRUMKIN, *Z. physik. chem.*, **A103,** 43 (1923); *Ergeb. exakt. Naturw.*, **7,** 235 (1928).
13. F. P. BOWDEN AND K. E. W. GREW, *Disc. Faraday Soc.*, **1,** 93 (1947).

The Difference Effect on Titanium Dissolving in Hydrofluoric Acid[1]

M. E. Straumanis and P. C. Chen

Department of Metallurgy, University of Missouri, School of Mines and Metallurgy, Rolla, Missouri

ABSTRACT

The difference effect was determined during the dissolution of commercial titanium coupled with platinum in 0.1, 0.24, 0.5, 1.0, and 2*N* hydrofluoric acid. The difference effect was directly proportional to the galvanic current up to 40 or 60 ma/cm², being nearly independent of concentration of the acid. At higher current densities the proportionality constant decreased. All the properties of the difference effect could be explained on the basis of the theory of local elements. Thus, the dissolution of titanium in hydrofluoric acid is an electrochemical process. The difference effect enables one to determine the degree of polarization of local elements formed on different metals.

Introduction

The difference effect was first observed by Thiel and Eckell (1). They found that the rate of hydrogen evolution from zinc in sulfuric acid or in hydrochloric acid decreased when it was polarized anodically. It can be observed that the rate of hydrogen evolution V_1 decreases to V_2 as soon as the zinc is connected electrically with a platinized platinum electrode, both electrodes being immersed in the same acid and in the same vessel. Then the difference effect is defined as:

$$\Delta = V_1 - V_2. \qquad \text{(I)}$$

The total rate of dissolution is higher than V_1, because the low overvoltage platinum electrode caused an additional current. The effect Δ is proportional[2] to this current as measured in the external circuit (see Fig. 3):

$$\Delta = KI. \qquad \text{(II)}$$

The correctness of this equation has been confirmed by several investigators (2–4), including, Streicher (5) who worked with aluminum in basic solutions.

It was shown that equation (II) can be derived on the basis of the theory of local elements (2). Conversely, the presence of the difference effect during the dissolution of a metal must prove that the dissolution occurs because of the activity of local cells.

Titanium dissolves quickly in hydrofluoric acid and it was shown by the authors (6) that this process is electrochemical in nature. Further proof in favor of the electrochemical concept is the establishment of the difference effect. This effect also permits study and measurement of polarization of a metal in a given solution.

Experimental Procedure

The apparatus for a measurement of the difference effect was arranged so that three determinations could be made successively, usually in one minute intervals. These determinations were: (*a*) the rate of dissolution of titanium in hydrofluoric acid from the hydrogen gas evolved, (*b*) the current between titanium and a platinum electrode, and (*c*) the emf between the dissolving titanium electrode and a calomel reference electrode.

The titanium electrode was prepared from Remington Arms 99 per cent titanium sheet by a previously described technique (6). The electrode was embedded in Bakelite with 2 cm² of surface exposed. The auxiliary platinized platinum electrode had the same surface area.

These two electrodes, the capillary tube for the potential measurements, and the stirring mechanism were assembled in the 200 ml flask as shown in Fig. 1. The inside wall of the flask and the outside of the capillary tube for potential measurement were coated with paraffin. The tube was an agar-1*N* KCl bridge. The flask was airtight when all stoppers were in place and stopcocks closed. The arrangement of the electrodes in the flask is shown in Fig. 1 and the electrical connections are shown in Fig. 2. The surfaces of the two electrodes were set about 2 mm apart with the tip of the capillary tube pressed tightly onto the surface of the titanium electrode.

The flask was immersed up to the line shown on Fig. 1 in a water bath held at 25° ± 0.1°C (6). The titanium electrode remained stationary while the acid was stirred. After displacing the air within the vessel with nitrogen (99.9%) for a period of 15

[1] Manuscript received February 27, 1951. This paper prepared for delivery before the Detroit Meeting, October 9 to 12, 1951.

[2] Regardless of the units in which the rate of dissolution is expressed.

minutes, 160 ml of hydrofluoric acid were poured into the flask through funnel g (Fig. 1) so that the titanium and platinum electrodes were completely covered by the acid. The stopcocks were then closed

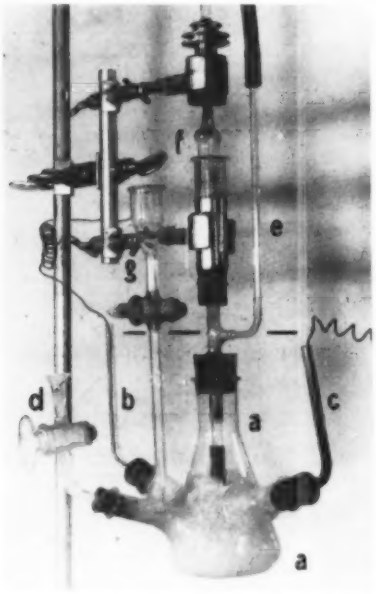

FIG. 1. Apparatus for the study of the difference effect: a—flask with paraffin lining, b—Pt electrode, c—Ti electrode, d—capillary tube from calomel cell, e—tube to gas buret, f—stirrer with Hg closure, g—funnel for introducing the acid.

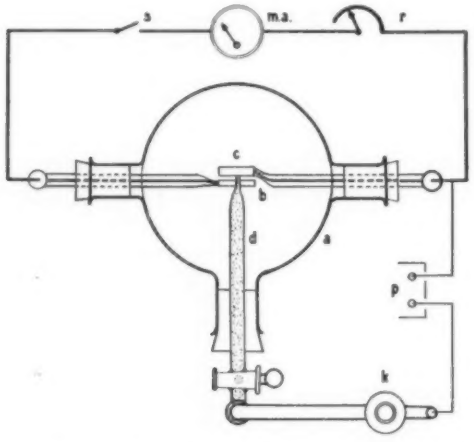

FIG. 2. Section through the lower part of Fig. 1, top view, stirring mechanism removed: k—calomel cell, p—potentiometer, r—variable resistance, m.a.—milliammeter, s—switch.

and the rate of dissolution of the titanium was recorded by measurement of the evolved hydrogen. Then the switch, s (Fig. 2), was closed, and the current was immediately adjusted to 2.5 or 5 milliamp/cm² by varying the resistance, r. With the circuit closed, the rate of dissolution was observed at regular intervals. The circuit was opened and the hydrogen evolution of uncoupled titanium V_1 was determined. Then the rate was determined at a higher current density. The same procedure was repeated until the maximum current that could be derived from the cell was reached. At the higher current densities the current was not steady.

Calculation of the Results

To calculate the difference effect, three factors are necessary: (*a*) V_1, the rate of hydrogen evolution from the freely corroding titanium, (*b*) V_t, the rate of total hydrogen evolution from the Ti-Pt couple, and (*c*) the rate of hydrogen evolution resulting from the current flowing in the Ti-Pt couple:

$$V_2 = k_1 I. \qquad \text{(III)}$$

The total rate is then:

$$V_t = V_2 + V_3.$$

From equations (I) and (III) it follows:

$$\Delta = V_1 + k_1 I - V_t. \qquad \text{(IV)}$$

Since $V_1 + k_1 I > V_t$ the difference has a positive value, and it shows the amount by which the rate of hydrogen evolution on titanium under the action of the current I is decreased. If this rate is expressed in $mm^3 cm^{-2} min^{-1}$, equation (IV) becomes:

$$\Delta = V_1 + 6.97\, I - V_t \qquad \text{(V)}$$

since one milliampere minute produces 6.97 mm³ hydrogen at standard conditions.

Combining equations (II) and (V) the slope constant k of equation (II) can be calculated at every current I.

RESULTS

Table I shows the values of the difference effect calculated from V_1, I, and V_t which were obtained by direct measurements in 0.5*N* hydrofluoric acid. For the calculation of the rate V_1, the average values between two adjacent zero current density readings were used. The total rate V_t was an average value obtained during the dissolution period of 20 minutes. The last two columns of the table show the linear relationship between the difference effect and the current density. The straight line goes through the origin of the coordinates. At higher current densities Δ declines slightly from the straight line equation. The maximum current density that could be drawn from the Ti-0.5*N* HF-Pt cell was 35.8 ma/cm².

Three determinations of the difference effect were made in 0.5*N* acid and one determination was made in each of the following concentrations of hydrofluoric acid: 0.1*N*, 0.24*N*, 1*N*, and 2*N*. The results are summarized in Fig. 3.

TABLE I. *Difference effect on Ti in 0.5N HF; 25°C. Hydrogen volumes reduced to normal conditions*

Time min	V_1 mm³/cm² min	I ma/cm²	6.97 I mm³/cm² min	V_t mm³/cm² min	Δ mm³/cm² min	k mm³/ma min
0	0	—	—	—	—	—
30	297	0	—	—	0	0
50	293	0	—	—	0	0
60	—	5.0	35	306	29	5.8
70	—	5.0	35	302		
80	302	0	—	—	0	0
90	—	10.1	70	314	62	6.1
100	—	10.1	70	306		
110	302	0	—	—	0	0
120	—	14.8	103	314	86	5.8
130	—	14.8	103	319		
140	297	0	—	—	0	0
150	—	20.0	139	323	113	5.7
160	—	20.0	139	314		
170	289	0	—	—	0	0
180	—	24.3	169	323	133	5.5
190	—	24.3	169	327		
200	289	0	—	—	0	0
210	—	29.3	204	344	149	5.1
220	—	29.3	204	340		
230	285	0	—	—	0	0
240	—	35.8	250	369	174	4.9
250	—	35.8	250	352		

TABLE II. *Slope constant k of the difference effect equation (II) obtained in various concentrations of HF at different current densities*

I ma/cm²	Concentration of hydrofluoric acid in *N*							k avg mm³/ma min
	0.1	0.24	0.5	0.5	0.5	1	2	
2.5	6.0	6.8	—	—				6.4
5.0	3.9	4.4	5.8	5.4	7.4	9.0	5.4	6.0
7.7	4.8	—	—	—	—	—	—	—
8.4	5.0	—	—	—	—	—	—	—
10		5.7	6.1	5.8	5.4	4.9	6.0	5.7
15		5.6	5.8	5.7	5.3	4.6	7.6	5.8
20			5.7	5.1		5.2	6.4	5.6
25			5.5	5.8		5.8	6.7	6.0
30			5.1	5.4		5.8	6.0	5.6
35			4.9			5.4	5.3	5.2
40						—	5.3	5.3
45						5.3	4.8	5.1
50						—	4.5	4.5
60						5.0	—	5.0
73.5							5.1	5.1
120							(4.3)	(4.3)
Average k	4.9	5.6	5.6	5.5	6.0	5.7	5.7	

It appears from Table II that the averaged difference effect is slightly smaller in the 0.1*N* acid than the average of 5.7 noted from the other acid concentrations. Table II shows further that the difference effect increases linearly with the current density up to 60 ma/cm². Above this the increase is less pronounced.

Potential measurements of dissolving titanium during the study of the difference effect were difficult because the vibration of the flask caused by the stirring mechanism aggravated the readings. However, a successful series of measurements was obtained in a 0.5*N* acid solution. This curve resembles one obtained at the dissolution of zinc in sulfuric acid (7) and is best fitted by a straight line.

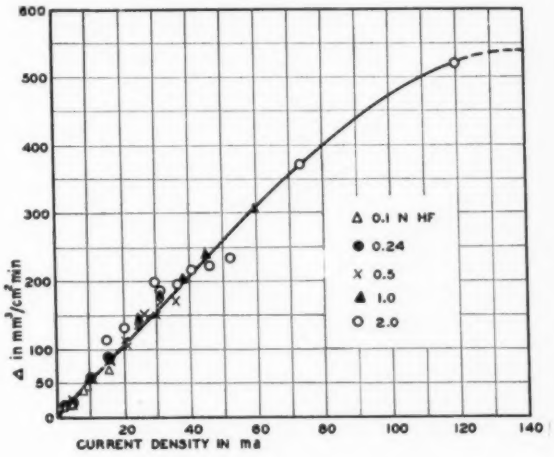

FIG. 3. Difference effect on Ti vs. current density in five different HF concentrations at 25°C.

Discussion

The meaning of the slope constant $k = 5.7$ of equation (II) is that the rate of hydrogen evolution on titanium is retarded by 5.7 $mm^3cm^{-2}min^{-1}$ for each milliampere of the current discharged through the platinum cathode. Therefore, the current necessary for the suppression of the hydrogen evolution on the titanium plate can be calculated from

$$I = \frac{V_1}{k} \qquad \text{(VI)}$$

since at that moment $V_1 = \Delta$. For instance, the hydrogen evolution rate from titanium in 0.24*N* hydrofluoric acid is 144 $mm^3cm^{-2}min^{-1}$. This practically ceases at a current density of 24.6 ma. However, Table II shows that the maximum current obtained in this acid was only 15 ma. Complete suppression of the hydrogen evolution was not achieved by current produced by the titanium-platinum couple. It might be that this is more nearly

possible by applying an auxiliary external current as shown by Streicher in the case of dissolution of aluminum in sodium hydroxide solutions (5).

By combination of equations (II) and (IV):

$$kI = V_1 + k_1 I - V_t. \qquad \text{(VII)}$$

Since $k = 5.7$ for concentrations between 0.2 and 2N and for current densities up to 40 ma/cm², the difference $V_t - V_1$ can be computed from:

$$\left.\begin{aligned} V_t - V_1 &= (k_1 - k)I \\ V_t - V_1 &= 1.27\ I \end{aligned}\right\} \qquad \text{(VIII)}$$

Equation (VIII) indicates that instead of 6.97 mm³ ($= k_1$) only 1.27 mm³ hydrogen are developed by one ma/cm² on the cathode per minute: approximately four-fifths of the current produced by the Ti-Pt couple is used to overcome the difference

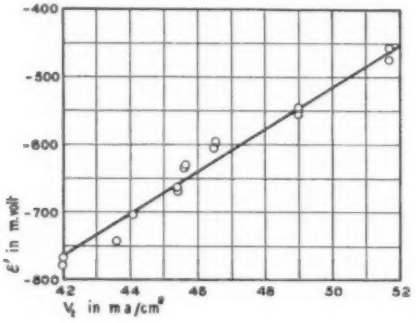

FIG. 4. Electrode potential of Ti measured under current in 0.5N HF. The total rate of hydrogen evolution V_t is converted into current.

effect and only one-fifth of it participates in the increase of the velocity of dissolution of titanium. At higher current densities the outcome is better because the constant k decreases (Table II).

The constant of equation (II) allows comparison of the magnitude of the difference effects obtained on different metals. For instance, in the case of dissolution of zinc in 2N sulfuric acid (8) an average constant of 2.5 was calculated (up to 73 ma/cm²). Approximately one-third of the current went to compensate the difference effect and two-thirds of the current contributed to the rate of dissolution of zinc [equation (VIII)]. Thus, the local elements on titanium (especially the anodes) are more readily polarized by an anodic current than those formed on zinc. This also contributes to the explanation of corrosion resistivity of titanium. It is apparent that k changes its value from metal to metal, and also as the electrolyte is changed. The highest value that can be reached by k is of $k = k_1$. In this case, equation (VII) shows that $V_1 = V_t$, which means that the rate caused by the current is completely subdued by the difference effect. On the other hand, if $k = 0$, there is no difference effect at all. The real cases are between these two extremes, assuming that no secondary processes, such as formation and breakdown of protective layers, occur during the anodic polarization on the anode. In Table II there are some k-values that exceed 6.97: they might be caused by experimental errors or by some changes occurring on the surface of titanium during the dissolution.

The difference effect can be explained under the following assumptions: (*a*) the dissolution of titanium in hydrofluoric acid is caused by the activity of local elements; (*b*) the potential of titanium vs. anodic current density varies linearly, as shown in Fig. 4 and as found in the case of other metals by Evans (9), Mears (10), Brown (11), and Streicher (12); and (*c*) the hydrogen overvoltage of the local cathodes is determined by the local current in accordance with the logarithmic overvoltage function. Straumanis has shown (2) that under these conditions the derivation of equation (II) for the difference effect was possible. Further, all the properties of the effect, observed in the case of titanium, follow from the theory given there. Even the decrease of the slope constants k with increasing current density (Fig. 3) can be explained [which is not possible with the pore theory of W. J. Müller (13)].

The dependence of the slope constant k [equation (II)] on concentration of the acid is also given by the equations for the effect (2). However, no large variations of the constant can be expected because the entire range of k-values lies between 0 and 6.97, as already pointed out. From the theory, the variation of k with the concentration might be expected to be larger, but the present data do not show any such real effect. Nevertheless, the experiments and the discussion confirm the opinion that dissolution of titanium in hydrofluoric acid is an electrochemical process and proceeds due to the activity of local elements.

Any discussion of this paper will appear in a Discussion Section, to be published in the June 1952 issue of the JOURNAL.

REFERENCES

1. A. THIEL AND J. ECKELL, *Z. Elektrochem.*, **33,** 370 (1927).
2. M. STRAUMANIS, *Z. physik. Chem.*, **A148,** 349 (1930); *Korrosion u. Metallschutz*, **14,** 67 (1938).
3. W. J. MÜLLER AND E. LÖW, *Z. Elektrochem.*, **42,** 790 (1936).
4. W. O. KROENIG AND V. N. USPENSKAJA, *Korrosion u. Metallschutz*, **12,** 130 (1936).

5. M. A. Streicher, *J.* (*and Trans.*) *Electrochem. Soc.*, **93**, 304 (1948); "Pittsburgh International Conference on Surface Reactions," Corrosion Publishing Co., Pittsburgh (1948).
6. M. E. Straumanis and P. C. Chen, *J. Electrochem. Soc.*, **98**, 234 (1951).
7. M. Straumanis, *Z. physik. Chem.*, **A147**, 173 (1930).
8. M. Straumanis, *Korrosion u. Metallschutz*, **14**, 71 (1938).
9. U. R. Evans, "Metallic Corrosion, Passivity and Protection," p. XXXIV, Longmans, Green & Co., New York (1948).
10. R. B. Mears, *J.* (*and Trans.*) *Electrochem. Soc.*, **95**, 1 (1949); R. B. Mears and R. H. Brown, *J. Electrochem. Soc.*, **97**, 75 (1950).
11. R. H. Brown, G. C. English, and R. D. Williams, *Corrosion*, **6**, 186, 1950.
12. M. A. Streicher, *J.* (*and Trans.*) *Electrochem. Soc.*, **96**, 170 (1949).
13. W. J. Müller, *Z. Elektrochem.*, **42**, 830 (1936); W. J. Müller and E. Löw, *Z. Elektrochem.*, **42**, 789 (1936); W. J. Müller, *Trans. Electrochem. Soc.*, **76**, 167 (1939).

The Zirconia-Yttria System[1]

Pol Duwez, Frank H. Brown, Jr., and Francis Odell[2]

Jet Propulsion Laboratory, California Institute of Technology, Pasadena, California

ABSTRACT

The phase relationships in the zirconia-yttria system have been established up to 2000°C. The addition of 0 to 5 mole per cent yttria lowers the temperature at which zirconia transforms from the tetragonal to the monoclinic form. From 7 to 55 mole per cent yttria is soluble in zirconia and this solid solution is cubic (stabilized zirconia). A two-phase region appears between 55 and 76 mole per cent yttria. With more than 76 per cent yttria, zirconia is soluble in yttria. These phase boundaries refer to the specimens rapidly cooled from 2000°C. The effect of lowering the temperature to 1375°C is to increase the width of the two-phase region between cubic zirconia and yttria solid solution. A tentative phase diagram of the zirconia-yttria system is presented.

The mechanism of stabilization of zirconia by an oxide of the yttria type is discussed in relation to the crystal structure of these two oxides. It is concluded that scandia, as well as other oxides of the rare earth group from element 62 to element 71, should stabilize zirconia by the same mechanism. Experimental results obtained on scandia, gadolinia, and samaria indicate that, as for yttria, the minimum amount of these oxides necessary to produce stabilization is about 6 mole per cent.

Introduction

The effect of yttria on the transformation of zirconia from the high temperature tetragonal to the room temperature monoclinic form has been investigated by Ruff and Ebert (1), and by Geller and Yavorsky (2). These investigations demonstrated the fact that if a sufficient amount of yttria is combined with zirconia, a stable cubic form of zirconia solid solution is obtained which is free from the large volume changes resulting from the allotropic transformation in pure zirconia. The purpose of the present study was to obtain more definite information on the minimum amount of yttria required for stabilization and to gain a better understanding of the phase relationships in the zirconia-yttria system.

Preparation of Samples and Methods of Measurements

The compositions of the specimens investigated are listed in Table I. The zirconia powder used[3] has been reported to have less than 1 per cent impurities (3). The particle size of the powder is less than 325 mesh, and a large fraction is probably less than 10 microns. The yttria powder[4] contains 0.7 per cent rare earth oxides of the yttrium group, 0.3 per cent rare earth oxides of the cerium group, and traces of iron.

The various compositions were prepared by mixing the powders, pressing at 20,000 psi, and firing for 2 to 6 hr at 2000°C in an oxyacetylene furnace (4). No chemical analysis of the specimens was made after firing. However, several specimens were weighed before and after firing, and since the change in weight was found to be less than a few tenths of 1 per cent, it was assumed that the change in composition was negligible.

The thermal expansion measurements were performed in an automatic recording dilatometer, described previously (5). All measurements were obtained with a rate of heating of 230°C/hr and a rate of cooling of 330°C/hr.

The structure of the various compositions was determined by x-ray diffraction. Powder patterns were taken using copper radiation filtered through a nickel foil and a camera having a diameter of 143.2 mm. The readings were corrected for film shrinkage. For lattice parameter computations the least squares method was applied to large angle reflections. Since the expected accuracy in lattice parameter was not more than one part in 4000, no correction was applied for absorption.

Crystal Structure of Zirconia and Yttria

The present knowledge of the crystal structure of zirconia has been discussed recently (6). The room temperature form is monoclinic with $a = 5.16$ kx, $b = 5.25$ kx, $c = 5.29$ kx, and $\beta = 80° 10'$. Above 1000°C the stable form is tetragonal with $a = 5.074$ kx and $c = 5.160$ kx. Both crystalline forms

[1] Manuscript received March 2, 1951. This paper prepared for delivery before the Washington Meeting, April 8 to 12, 1951.

[2] Present address: Surface Alloys, Inc., Los Angeles, California.

[3] Grade A Zirox from the Titanium Alloy Manufacturing Division, National Lead Company, Niagara Falls, New York.

[4] From Research Chemicals, Inc., Burbank, California.

are slightly distorted cubic structures of the CaF_2 type. Another high temperature form, reported by Cohn (7), has never been confirmed and is not considered in the present study.

TABLE I. *Results of measurements on zirconia-yttria compositions*

Yttria content		Phases present
mole %	weight %	
0	0	Monoclinic, $a = 5.16$ kx, $b = 5.25$ kx, $c = 5.29$ kx, $\beta = 80° 10'$
1	1.82	Monoclinic
2	3.61	Monoclinic
3	5.36	Monoclinic
4	7.09	Weak monoclinic and cubic not resolved
5	8.80	Very weak monoclinic and cubic not quite resolved
7	12.06	Cubic resolved, $a = 5.115$ kx
10	19.29	Cubic resolved, $a = 5.122$ kx
15	24.44	Cubic resolved, $a = 5.141$ kx
20	31.42	Cubic resolved, $a = 5.153$ kx
25	37.92	Cubic resolved, $a = 5.165$ kx
30	43.99	Cubic resolved, $a = 5.181$ kx
40	54.99	Cubic resolved, $a = 5.203$ kx
50	64.70	Cubic resolved, $a = 5.219$ kx
55	64.70	Cubic resolved, $a = 5.230$ kx
60	73.33	Cubic, $a = 5.232$ kx, and weak yttria solid solution
65	77.29	Cubic, $a = 5.230$ kx, and yttria solid solution
70	81.05	Cubic, $a = 5.231$ kx, and yttria solid solution, $a = 10.542$ kx
75	84.61	Very weak cubic and yttria solid solution, $a = 10.541$ kx
80	88.00	Yttria solid solution, $a = 10.548$ kx
90	94.28	Yttria solid solution, $a = 10.564$ kx
100	100	Yttria, $a = 10.586$ kx

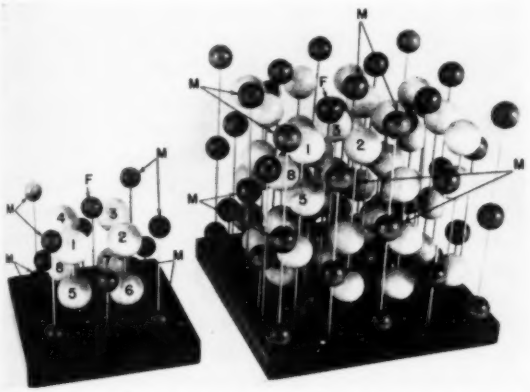

FIG. 1. Unit cells of cubic zirconia and yttria. One eighth of the unit cell of yttria, limited by the metal atoms marked M, is similar to the zirconia cell, except for (*a*) a small shift in the position of the metal atom on the face of the cube (one out of six of these atoms is marked F), (*b*) removal of oxygen atoms corresponding to No. 4 and 6 in the zirconia structure, and (*c*) a slight shift in the position of the remaining six oxygen atoms, marked 1, 2, 3, 5, 7, and 8.

The crystal structure of yttria is body-centered cubic (Tl_2O_3 type). The unit cell contains 80 atoms (48 oxygen and 32 yttrium) in special positions of the space group $Ia3 - T_h^7$. The coordinates of the atoms have been tabulated (8). Although the structure of yttria looks very complex at first, it bears some resemblance to that of cubic zirconia (CaF_2 type). The unit cell of yttria may be considered (8)

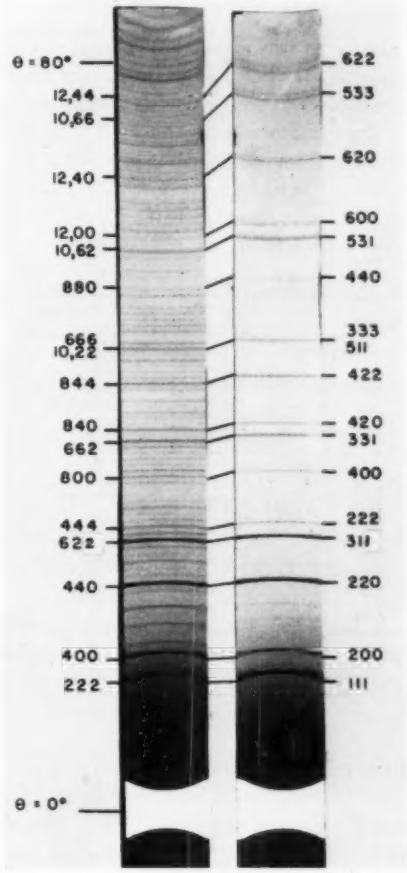

FIG. 2. Powder patterns of cubic zirconia solid solution (40 mole per cent yttria) and of yttria solid solution (10 mole per cent zirconia).

as made up of eight cells of zirconia in which the trivalent metal yttrium replaces zirconium atoms and only three fourths of the oxygen positions are occupied. As a result of the vacancies left by the missing oxygen, both metal and oxygen atoms are slightly shifted from the positions they occupy in zirconia and the atomic arrangement is relatively more complicated. The complication, however, is mostly due to the special positions occupied by the oxygen atoms. The metal atoms are not displaced very much, 8 being in positions they would occupy in cubic zirconia, and the 24 remaining atoms being

displaced a distance equal to only 3 per cent of the edge of the unit cell.

By constructing models of the unit cells of the two oxides, it is possible to visualize how closely related these structures are. Photographs of such models are reproduced in Fig. 1. Although the lack of perspective prevents showing clearly the slight shifts in the position of the metal atoms, the difference in the number and the position of the oxygen atoms is quite apparent.

The similarity between the crystal structure of cubic zirconia and that of yttria is also reflected in the appearance of the x-ray diffraction patterns of the two oxides. Since some of the metal atoms in both structures have the same positions in space, some of the reflections are the same in the powder patterns of the two structures, except for a shift due to the difference in the size of the unit cell. In

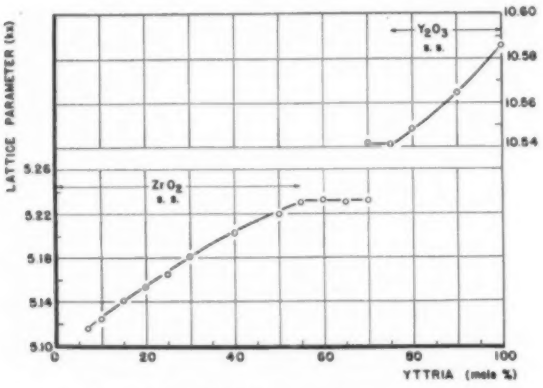

FIG. 3. Variation of lattice parameter of cubic zirconia and yttria solid solutions with yttria content.

fact, all the reflections of cubic zirconia (made cubic by the addition of yttria in solid solution) are present in the powder pattern of yttria. The indices of these equivalent reflections are in the ratio 1:2, so that a (111) reflection in cubic zirconia, for example, is equivalent to a (222) reflection in yttria. The equivalence between the two patterns is illustrated in Fig. 2. The extra reflections in yttria are, of course, due to planes containing atoms which are not in the same positions they would occupy in the zirconia structure. The importance of recognizing the similarity between the crystal structures of zirconia and yttria will become apparent in the discussion of the phase relationships in this system.

Results of X-Ray Diffraction Measurements on Zirconia-Yttria Compositions

Compositions given in Table I were fired for 2 hr and allowed to cool in the furnace. The rate of cooling was such that the temperature dropped from 2000° to 1400°C in about 10 min. This rate of cooling is sufficiently rapid to prevent any appreciable change in concentration by diffusion in the solid state and only the rapid allotropic change from the tetragonal to the monoclinic zirconia could take place. It was therefore assumed that, with the exception of the tetragonal-monoclinic inversion, the structure of the specimens at room temperature was that prevailing at 2000°C.

A second series of specimens which had been subjected to the same firing schedule was subsequently heated for 336 hr at 1375°C. The results of the study of the structure of these two series of specimens will be analyzed separately.

Specimens Fired at 2000°C

The results of x-ray diffraction measurements made on these specimens are summarized in Table I. Up to 3 mole per cent yttria, only the monoclinic phase is present. It is probable that within this range of composition, yttria is soluble in tetragonal zirconia at high temperature and is retained in solution in the monoclinic form after cooling. In order to prove this statement, it would suffice to show that the size of the unit cell of zirconia is progressively increased by the addition of yttria. Unfortunately, a small variation in the lattice parameter of monoclinic zirconia is difficult to detect, because the powder pattern of monoclinic zirconia does not have sharp reflections at high Bragg angles. It is therefore almost impossible to detect the small variation in cell size that would accompany the presence of less than 3 per cent yttria in solid solution.

In the specimens containing 4 and 5 mole per cent yttria, two phases were observed, namely monoclinic and cubic zirconia, the amount of cubic zirconia increasing with yttria content (cf. Table I). The high angle reflections of the cubic phase, however, were not sharp enough to give reliable values of lattice parameters. For yttria content varying from 7 to 55 mole per cent, a single cubic x-ray diffraction pattern with sharply resolved doublets indicated clearly that these specimens contained only one phase, consisting of a solid solution of yttria in zirconia. In this range of composition, the lattice parameter of the cubic phase varies almost linearly, as required by Vegard's law (cf. Fig. 3).

From 55 to 75 mole per cent yttria, the specimens contained two phases, one having the cubic zirconia structure and the other the yttria structure. Judging from the relative intensities of the diffraction patterns of the two phases, it was evident that the amount of the yttria phase increased steadily with increasing percentages of yttria. In this two-phase region, the lattice parameters of both phases should

remain constant. The results shown in Fig. 3 indicate that this condition is satisfied.

From 80 mole per cent yttria to pure yttria, the specimens contained a single phase having the yttria structure. The fact that within this composition range zirconia is soluble in yttria is illustrated by the almost linear variation in lattice parameter with concentration (cf. Fig. 3).

Samples Reheated for 336 Hours at 1375°C

In order to gain additional information on the effect of temperature on the phase boundaries, a series of specimens having the same compositions as those given in Table I was reheated for 336 hr at 1375°C. After this treatment, the only changes in structures occurred in the specimens containing

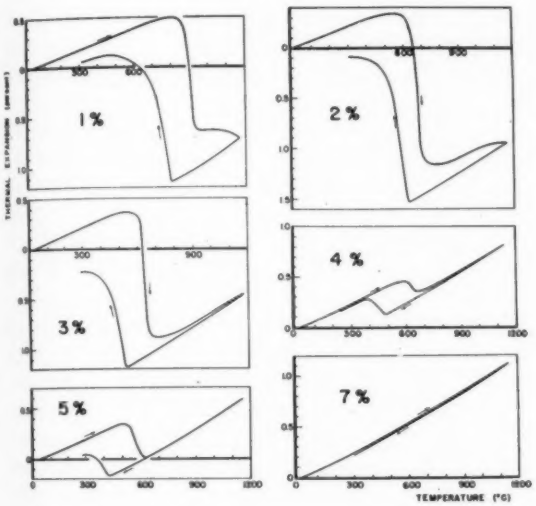

FIG. 4. Linear thermal expansion curves of zirconia containing various mole percentages of yttria.

55 and 80 mole per cent yttria. These two specimens, which after cooling from 2000°C were cubic zirconia solid solution and yttria solid solution, respectively, contained both zirconia and yttria solid solutions. This result indicates that the extent of the two-phase regions is greater at 1375°C than at 2000°C. In other words, the solubility of yttria in zirconia and of zirconia in yttria decreases with decreasing temperature.

THE TETRAGONAL-MONOCLINIC INVERSION MEASURED BY THERMAL EXPANSION

The tetragonal to monoclinic allotropic change in pure zirconia is accompanied by a large volume change. By measuring the change in length of a specimen during heating and cooling, it is possible to determine the temperature at which the transformation takes place. This method, used by several investigators (2, 3), was applied to specimens containing less than 7 mole per cent yttria. Typical thermal expansion curves are reproduced in Fig. 4. The curve obtained for pure zirconia is similar to those previously published (2). Contraction due to the monoclinic to tetragonal transformation on heating is rather progressive, whereas expansion accompanying the reverse transformation on cooling is sharply defined. Consequently, the temperature at which transformation takes place on cooling is generally taken as representative.

The relation between transformation temperature on cooling and yttria content is shown in Fig. 5. The transformation temperature is lowered with increasing yttria content and at 7 mole per cent yttria or more no transformation takes place. These results are in agreement with the work of Geller and Yavorsky (2), who reported that the transformation temperature for specimens containing 4.5 mole per

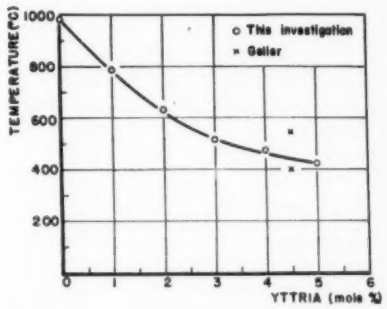

FIG. 5. Effect of yttria on the transformation temperature from tetragonal to monoclinic zirconia on cooling [Geller (2)].

cent yttria is between 400° and 500°C and that no transformation occurs in specimens containing 8.8 mole per cent yttria.

PHASE RELATIONSHIPS IN THE ZIRCONIA-YTTRIA SYSTEM

Since measurements performed in the present investigation were concerned only with changes in structure of zirconia-yttria bodies in the solid state, it is impossible to establish a complete equilibrium diagram. The results obtained, however, are sufficient to outline the diagram for temperatures below 2000°C and to construct tentative solidus-liquidus boundaries that would be compatible with the experimental evidence. Such a diagram is presented in Fig. 6. The solid state phase boundaries have been drawn to account for the following experimental results previously discussed:

1. Solid solution of yttria in tetragonal zirconia from 0 to about 6 mole per cent.

2. Transformation of this solid solution into a

monoclinic zirconia solid solution along a line taken from Fig. 5.

3. A one-phase region of cubic zirconia solid solution extending from 7 to 56 mole per cent at 2000°C and from 7 to about 52 mole per cent at 1375°C.

4. A two-phase region between the tetragonal and the cubic zirconia solid solution. In order to satisfy the phase rule, the existence of this two-phase region was assumed without actual experimental proof. It was also assumed that a eutectoid reaction takes place at about 400°C. This assumption, which leads to the existence of a narrow two-phase region between monoclinic and cubic zirconia, is compatible with the fact that monoclinic and cubic zirconia were present in specimens containing 4 and 5 mole per cent yttria.

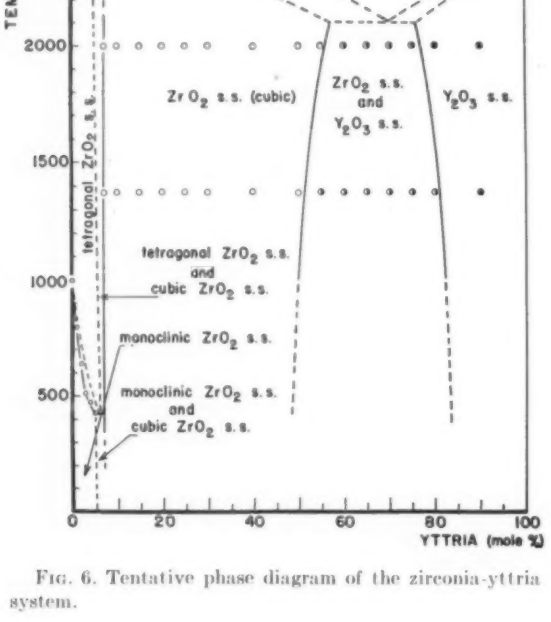

FIG. 6. Tentative phase diagram of the zirconia-yttria system.

5. A two-phase region containing cubic zirconia solid solution and yttria solid solution and extending from 56 to 77 mole per cent yttria at 2000°C and from 52 to approximately 82 mole per cent yttria at 1375°C.

6. An yttria solid solution field extending from 77 mole per cent yttria at 2000°C and from 82 mole per cent yttria at 1375°C.

The phase boundaries above 2000°C, shown by dotted lines in Fig. 6, are only tentative. The shape given to the diagram in this region is the simplest possible one. The peritectic reaction, located arbitrarily at 2500°C, is necessary in order to generate the one-phase cubic solid solution region. The existence of a eutectic, whose temperature was also located arbitrarily, seems to be the most logical assumption to explain the presence of a two-phase region between cubic zirconia and yttria.

The zirconia-yttria phase diagram presented in Fig. 6 is of a rather simple type. Except for the zirconia-rich portion, where phase boundaries are complicated because of the allotropic change in pure zirconia, the diagram between 7 and 100 per cent yttria is made of two solid solution regions separated by a two-phase region. Considering the fact that the two oxides do not have the same stoichiometric composition, it is rather surprising to find wide ranges of mutual solubility and no intermediate compound. It is well known that one of the conditions for the formation of solid solutions over wide ranges of concentrations is that the crystal structure of the two oxides be the same. The system zirconia-yttria appears to violate the generally accepted rules of solid solubility. It is not difficult, however, to show that this system may be considered as a border case to which the rules may be logically extended.

In the discussion of the crystal structure of zirconia and yttria given in a previous section of this paper, it was pointed out that the atomic arrangement in the two oxides is very nearly the same, and it is only because of a small shift in atomic positions that the two crystal structures belong to different space groups. Since in the formation of solid solutions the similitude in atomic patterns is the important condition, the mutual solubility of zirconia and yttria appears to be logical. However, some special features must also be present in the structures of the oxides in order to explain the formation of solid solutions between oxides having different stoichiometric ratios of metal to oxygen. In the case of solid solubility of an oxide of the MO_2 type (zirconia) with one of the M_2O_3 type (yttria), there is either a deficiency in oxygen when MO_2 is the solvent or an excess of oxygen when M_2O_3 is the solvent. These solid solutions are possible only if the crystal structure of the oxide of the MO_2 type is stable with vacant oxygen sites and if the crystal structure of the oxide of M_2O_3 type has "holes" that can be filled by the oxygen atoms in excess. These two conditions appear to be satisfied in the zirconia-yttria system.

Previous investigations have established that the oxides having the cubic CaF_2 structure (like zirconia) may lose an appreciable amount of oxygen and still retain their crystal structure. In a study of the ceria-lanthana system, Zintl and Croatto (9) have shown that ceria (CeO_2) can dissolve as much as 43

mole per cent of lanthana (La_2O_3), and in this solid solution range the parameter of ceria varies continuously from 5.396 to 5.586 Å. By making accurate density measurements, these investigators confirmed the theory that in a solid solution of this type, the number of unoccupied oxygen sites corresponds to the deficiency in oxygen resulting from the substitution of an M_2O_3 type of oxide for an MO_2 type. The results of the present investigation of the zirconia-yttria system are very similar to those of Zintl and Croatto on the ceria-lanthana system, and the explanation of the solid solubility of zirconia-yttria may be based on the formation of a zirconia lattice with vacancies due to oxygen deficiency. The existence of lattice vacancies may also be used as the basic reason for a solid solution of zirconia into yttria. In this case, the vacancies exist in the yttria crystal structure and the extra oxygen brought in by the zirconia can easily occupy the vacant sites.

Stabilization of Zirconia with Rare Earth Oxides

In order to gain a better understanding of the mechanism of stabilization of zirconia, it is important to know the phase relationships between zirconia and the stabilizing oxide. When such relationships are known for one oxide, it should be possible to predict what other oxides could stabilize zirconia by the same mechanism. The present investigation has shown that yttria-stabilized zirconia is a solid solution having a range of yttria concentration from 6 to about 50 mole per cent yttria. Other oxides which would form similar solid solutions should have the same stabilizing effect. These oxides would therefore be similar to yttria, the similitude referring to the factors governing the formation of solid solutions. The oxides similar to yttria are those of the elements No. 21 (scandium) and No. 62 to 71 (rare earths from samarium to lutecium). The metallic atoms in these oxides have the same electronic configuration as yttrium, since all possess two (s) and one (d) valence electrons. Their ionic diameters are very nearly the same (10), and they are structurally isomorphous with yttria (body-centered cubic, Tl_2O_3 type). It is therefore highly probable that the oxides will behave like yttria in their reactions with zirconia, and that, in particular, they will promote the stabilization of zirconia.

The experimental verification of the expected relationship between zirconia and the rare earth oxides was limited to those oxides that could be procured at reasonable cost and in sufficient quantity. Furthermore, the investigation was limited to the determination of the minimum amount of oxide necessary for stabilizing zirconia to the cubic form.

Three oxides of the yttria type were studied, namely, scandia, samaria, and gadolinia.[5] After they were fired at 2000°C in an oxidizing atmosphere, the structures were analyzed by x-ray diffraction. All lines of the powder patterns were readily indexed on the basis of a body-centered cubic structure and the following lattice parameters were determined: scandia, 9.788 kx; yttria, 10.586 kx; samaria, 10.845 kx; gadolinia, 10.790 kx. These parameters agree closely with literature values (11). The technique used for preparing the various specimens of zirconia with one of the three oxides was essentially the same as that described above for the zirconia-yttria specimens. The various percentages of oxides added to zirconia are given in Table II, together with the results of the x-ray investigation. These results reveal that by adding either scandia, samaria, or gadolinia to zirconia, it is possible to obtain the stable cubic form of zirconia. Furthermore, the minimum amount of oxide necessary to stabilize zirconia is in the neighborhood of 6 mole per cent, which is the value found previously for yttria. It is thereby demonstrated that four oxides of the yttria type have very similar effects on the stabilization of zirconia. A generalization of this similarity to all the oxides of elements No. 62 to 71 appears to be a safe extrapolation.

TABLE II. *Results of experiments on the stabilization of zirconia with scandia, samaria, gadolinia, and yttria*

Added oxide	Mole concentration (%)	Phases present	Lattice parameter of cubic zirconia phases
			kx
Scandia	4.5	Monoclinic and cubic	—
	5.5	Very weak monoclinic and cubic	—
	6.5	Cubic	5.071
	9.0	Cubic	—
Samaria	1	Monoclinic and very weak cubic	—
	2	Monoclinic and very weak cubic	—
	4.5	Weak monoclinic and cubic	—
	5.5	Very weak monoclinic and cubic	—
	6.5	Cubic	5.140
Gadolinia	3.5	Monoclinic and weak cubic	—
	5.8	Very weak monoclinic and cubic	—
	7.5	Cubic	5.136
Yttria	7.0	Cubic (cf. Table I)	5.115

An interesting study may be made of the variations in the lattice parameters of the cubic zirconia stabilized with the minimum addition of several

[5] These oxides were obtained from the Fairmount Chemical Company, New York.

oxides of the yttria type. The four parameters given in Table II for cubic zirconia increase in the sequence: scandia, yttria, gadolinia, and samaria. This is the order in which the lattice parameters of these four oxides also increase. The fact is that when these results are plotted on a graph, the relation between the cubic zirconia parameter and the parameter of the added oxide is almost linear. This is additional evidence that oxides of the yttria type stabilize zirconia into the cubic form by entering into solid solution in zirconia.

Conclusions

1. The addition of yttria to zirconia lowers the temperature at which zirconia transforms from the tetragonal to the monoclinic form, and no transformation occurs when the yttria concentration is above approximately 6 mole per cent.

2. At 2000°C, yttria and zirconia form solid solutions from 7 to 55, and from 76 to 100 mole per cent yttria, respectively. These two solid solutions are separated by a two-phase region extending from 55 to 76 mole per cent yttria. At 1375°C the only change in the phase relationship is a slight increase in the width of the two-phase region.

3. The solubility of the two oxides over rather wide ranges of concentrations is explained by the similitude in the atomic arrangements in the structures of the two oxides and by the fact that the cubic zirconia lattice is stable even when all the oxygen sites are not occupied, whereas the yttria lattice has vacant sites in which excess oxygen atoms can be located.

4. Oxides similar to yttria, namely scandia and all the rare earth oxides from elements No. 62 to 71, should exhibit the same properties as yttria when added to zirconia. Limited experimental evidence for this prediction is given by establishing that the minimum amount of scandia, samaria, and gadolinia necessary to form a cubic zirconia solid solution is 6 mole per cent, as in the case of yttria.

Acknowledgment

This work was done at the Jet Propulsion Laboratory, California Institute of Technology, under contract number W-04-200-ORD-455 with the Army Ordnance Department, Washington, D. C. The authors wish to thank this agency for the permission to publish the results of this investigation.

Any discussion of this paper will appear in a Discussion Section, to be published in the June 1952 issue of the Journal.

REFERENCES

1. O. Ruff and F. Ebert, *Z. anorg. Chem.*, **180,** 19 (1929).
2. R. F. Geller and P. J. Yavorsky, *J. Research Nat. Bur. Standards*, **35,** 87 (1945).
3. C. E. Curtis, *J. Am. Ceram. Soc.*, **30,** 180 (1937).
4. P. Duwez, F. Odell, and J. Taylor, *J. Am. Ceram. Soc.*, **32,** 1 (1949).
5. P. Duwez and H. Martens, *Trans. Am. Inst. Mining Met. Engrs.*, **185,** 571 (1949).
6. P. Duwez and F. Odell, *J. Am. Ceram. Soc.*, **33,** 274 (1950).
7. W. M. Cohn, *Trans. Electrochem. Soc.*, **68,** 65 (1935).
8. L. Pauling and M. D. Shappell, *Z. Krist.*, **75,** 128 (1930).
9. E. Zintl and U. Croatto, *Z. anorg. u. allgem. Chem.*, **242,** 79 (1939).
10. R. W. G. Wyckoff, "Crystal Structures," Chap. IV, p. 15, Interscience Publishers, Inc., New York (1948).
11. H. Bommer, *Z. anorg. u. allgem. Chem.*, **241,** 273 (1939).

Luminescence of Three Forms of Zinc Orthophosphate:Mn[1]

ARTHUR L. SMITH

Tube Department, Radio Corporation of America, Lancaster, Pennsylvania

ABSTRACT

Three forms of zinc orthophosphate:manganese have been found. The α form corresponds in x-ray diffraction pattern to the published values. The luminescence is green, the peak wavelength being 5540 Å. It is produced when manganese concentrations are below 1 mole per cent, or when higher concentrations are not heated above 700°C. The β form has a red luminescence with a peak at 6380 Å. This formation occurs at manganese concentrations above 1 mole per cent and firing temperatures above 800°C. The γ form may be produced by additions of magnesium orthophosphate above 3 mole per cent. The emission is similar to the β form with a peak at 6320 Å, and of somewhat lowered intensity.

INTRODUCTION

Zinc phosphates activated by manganese have been mentioned in the literature as exhibiting cathodoluminescence, but no detailed report on the orthophosphate as such has been found. A paper by Levy and West (1) indicated they had used "zinc orthophosphate:Mn," but gave no preparative or optical details except to state that the emission was "red" and of exponential decay. Henderson (2) later gave more definitive, but still incomplete, information about such a compound. He found the peak of emission to be dependent on the manganese concentration, shifting from 6300 Å at a concentration of 0.2 weight per cent to 6320 Å at 1.0 weight per cent. The only details of preparation were that the phosphors were prepared either by precipitation from solution or by heating zinc carbonate with ammonium phosphate, and that firing was carried out in the region of 900°C. Iwasé (3) prepared a number of samples of zinc orthophosphate with varying amounts of manganese. How they were prepared was not mentioned. He called their cathodoluminescence an "intense orange" and published a curve of the emission which peaked at 6700 Å and tailed slowly to 5100 Å. He did not mention any shift of color with varying manganese concentration. Recently Moskvin (4) precisely determined the color for a manganese-activated zinc orthophosphate and confirmed that it has an e^{-t} type decay. No further details were given. Kroeger (5) listed a series of zinc and zinc-alkali phosphates, the emission of which was termed orange to yellow-green.

Miller (6) reported that when zinc orthophosphate was doubly activated with lead and manganese a phosphor was obtained which, on excitation by 1850 Å radiation and stimulation by infrared radiation, gave a yellow emission. The base materials for these phosphors were precipitated by adding the theoretical amount of a neutral ammonium phosphate solution to a zinc chloride solution. After activation by $MnCl_2$ and $PbSO_4$ and the addition of Li_2SO_4 flux, the material was fired at 750°C "to incipient fusion."

This investigation of the $Zn_3(PO_4)_2$:Mn system has shown that there are three crystalline modifications possible. The first, which is identical in x-ray diffraction pattern with the published value (7) for zinc orthophosphate, we have labeled the α form. It occurs when no, or very little, manganese is incorporated into the structure. Cathodoluminescence of the manganese-activated structure is green (5520 Å) of moderate intensity, and of relatively short persistence. The second, or β form, occurs at higher manganese concentration ($>$ 1 mole per cent) and higher temperatures ($>$ 750°C). The x-ray diffraction pattern is quite distinct from that of the α form (Table I). The cathodoluminescence of this form is red (6380 Å), has double the peak intensity of the α form, and is of much longer persistence. The third, or γ form, is most easily obtained by small additions of magnesium (about 3 mole per cent), although many other additions serve as well. The emission of this form when activated by manganese is similar to the β form, but of somewhat lowered peak intensity.

The effects of other inclusions, such as pyrophosphate ion, addition of alkali ions, etc., were also determined. In general, they slowed the phase changes and hence gave products with emissions which were composites of the green and red bands. Double activation by lead and manganese was also briefly investigated, and infrared-stimulable phosphors were obtained.

EXPERIMENTAL

Preparation of Phosphors

Chemicals of C.P. or analytical reagent grade were found satisfactory in this investigation as reac-

[1] Manuscript received May 7, 1951. This paper prepared for delivery before the Washington Meeting, April 8 to 12, 1951.

TABLE I. *Diffraction data for α, β, and γ forms of zinc orthophosphate*

α Phase		β Phase		γ Phase	
Lattice spacing (*d*-) Angstroms	Estimated relative intensity	Lattice spacing (*d*-) Angstroms	Estimated relative intensity	Lattice spacing (*d*-) Angstroms	Estimated relative intensity
4.6	0.40	4.20	0.30	8.5	0.05
4.4	0.40	3.90	0.80	5.6	0.05
4.20	0.20	3.65	0.30	4.35	1.00
4.00	0.70	3.50	0.15	4.00	0.45
3.60	0.90	3.30	1.00	3.80	0.05
3.42	0.45	3.10	1.00	3.40	1.00
3.25	0.15	2.85	1.00	3.22	0.30
3.10	1.00	2.64	0.05	3.02	0.30
2.80	0.20	2.55	0.45	2.90	0.10
2.63	0.40	2.48	0.45	2.80	0.30
2.52	0.30	2.38	0.50	2.70	0.10
2.43	0.50	2.30	0.30	2.62	0.10
2.29	0.40	2.19	0.30	2.50	0.80
2.23	0.30	2.14	0.30	2.43	0.45
2.10	0.30	2.08	0.65	2.38	0.45
2.02	0.20	2.02	0.25	2.30	0.10
1.96	0.25	1.99	0.25	2.22	0.15
1.83	0.35	1.95	0.25	2.10	0.65
1.77	0.30	1.90	0.30	2.02	0.40
1.66	0.40	1.86	0.65	1.93	0.10
1.59	0.10	1.77	0.30	1.84	0.10
1.54	0.50	1.70	0.50	1.83	0.20
1.51	0.30	1.67	0.50	1.80	0.10
1.47	0.10	1.64	0.50	1.76	0.40
1.44	0.30	1.59	0.35	1.69	0.15
1.41	0.30	1.56	0.40	1.65	0.55
1.35	0.30	1.53	0.35	1.62	0.05
1.32	0.30	1.50	0.40	1.59	0.05
1.22	0.20	1.48	0.05	1.54	0.60
1.20	0.15	1.46	0.05	1.50	0.25
1.18	0.05	1.44	0.10	1.464	0.10
1.166	0.15	1.42	0.10	1.442	0.45
1.142	0.10	1.41	0.10	1.396	0.10
1.120	0.10	1.39	0.30	1.380	0.10
1.107	0.05	1.36	0.30	1.360	0.10
1.090	0.15	1.345	0.25	1.320	0.35
1.068	0.20	1.33	0.35	1.300	0.10
1.050	0.10	1.305	0.15	1.282	0.10
1.035	0.15	1.290	0.10	1.270	0.10
0.975	0.10	1.275	0.10	1.255	0.10
0.962	0.15	1.240	0.30	1.230	0.15
0.950	0.10	1.220	0.35	1.220	0.15
0.940	0.10	1.210	0.15	1.200	0.20
0.921	0.10	1.195	0.20	1.180	0.15
0.911	0.10	1.165	0.10	1.160	0.05
other faint lines		1.154	0.10	1.146	0.15
		1.140	0.10	1.140	0.10
		1.126	0.10	1.120	0.15
		1.105	0.10	1.108	0.20
		1.090	0.25	1.090	0.10
		1.074	0.15	1.080	0.10
		1.060	0.20	1.070	0.25
		1.050	0.20	1.054	0.05
		1.038	0.20	1.044	0.05
		1.031	0.10	1.031	0.15
		1.023	0.10	1.020	0.15
		1.016	0.20	1.010	0.15
		1.005	0.20	1.000	0.10
		0.995	0.05	0.998	0.10
		0.985	0.20	0.988	0.10
		0.970	0.30	0.980	0.10
		0.962	0.30	0.956	0.10
		0.956	0.30	0.945	0.10
		0.942	0.15	0.935	0.05
		0.929	0.15	0.931	0.15
		0.920	0.15	0.920	0.05
		0.914	0.05	0.912	0.10
		0.909	0.15	0.905	0.10
		0.900	0.30	0.900	0.05
		0.893	0.15	0.894	0.05
		0.886	0.05	0.888	0.20
		0.876	0.10	0.862	0.15
		0.860	0.20	0.854	0.15
		0.850 other lines	0.20	other lines	

tants. More highly purified materials did not produce an improved product.

A variety of reactions may be used to produce zinc orthophosphate, but most of these are unsuitable because the product either is contaminated with other compounds or cannot be handled conveniently. The method selected utilizes the reaction between a soluble zinc salt and disodium hydrogen orthophosphate. A pure product of proper physical characteristics is obtained if the *p*H of the final solution yielding the orthophosphate is less than 5. The yield is less than 100 per cent because of the solubility of $Zn_3(PO_4)_2$, even in dilute acids. Attempts to increase the yield by neutralizing the final solution with hydroxides give rise to foreign compounds. For example, in neutral or alkaline solutions

$$Na^+ + PO_4^{3-} + Zn^{2+} \rightarrow ZnNaPO_4 \downarrow$$

and

$$NH_4^+ + PO_4^{3-} + Zn^{2+} \rightarrow ZnNH_4PO_4 \downarrow .$$

The latter decomposes upon heating in the manner

$$2ZnNH_4PO_4 \rightarrow Zn_2P_2O_7 + 2NH_3 \uparrow + H_2O \uparrow .$$

The yield may be increased to 90 per cent of the theoretical amount by using a 50 per cent excess of Na_2HPO_4. It is possible to increase the yield still further by using greater excesses, but this step was not considered necessary. The crystal size and character of the precipitate may be regulated by control of the rate of mixing, the sequence of addition, and the temperature at which crystallization occurs.

The precipitate obtained by this method when

dried at 160°C is the hydrate $Zn_3(PO_4)_2 \cdot 2H_2O$, as confirmed by x-ray and chemical analysis. Upon heating, the α form of the orthophosphate is obtained.

In the early part of the work, when activator concentrations were under study, manganese sulfate was added in solution, and the slurry dried at 150°–200°C. Later, however, manganese phosphate was coprecipitated directly with zinc orthophosphate. A much more homogeneous product is thereby obtained and subsequent handling is eliminated. The greater solubility of manganese phosphate requires that manganese be added in an amount larger than theoretically necessary. The correct proportion was determined empirically, no study having been made of relative solubility.

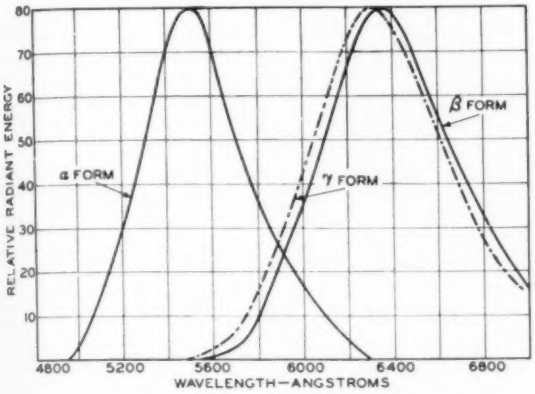

FIG. 1. Spectral energy emission characteristics of α, β, and γ forms plotted with equal peak radiations.

Firing was conducted in open shallow quartz trays in a muffle furnace. The temperature range investigated was between 600°–1100°C.

Testing of Phosphors

Cathodoluminescent efficiencies and emission spectra were determined by using a defocused electron beam with a current density of 1.5 $\mu a/cm^2$ and an accelerating potential of 8000 v. Peak efficiencies and spectral distribution of energy were measured by means of the spectroradiometer and the method described by A. E. Hardy (8). The visual efficiencies were determined with an eye-corrected photocell. Radiation in the 1850 Å region was obtained by removing the filter from a "Mineralight," which contains a mercury lamp in a quartz envelope.

Results

Zinc orthophosphate without any manganese addition does not show any phase change even up to the point of fusion. At all temperatures the x-ray diffraction pattern corresponds to the α form. This phase persists when manganese is added so long as the manganese concentration is less than 0.75 mole per cent. The cathodoluminescence of the manganese-activated α form is green, the peak emission occurring at 5520 Å (Fig. 1). As the manganese concentration is increased, the shape and the location of the peak of the emission curve remain un-

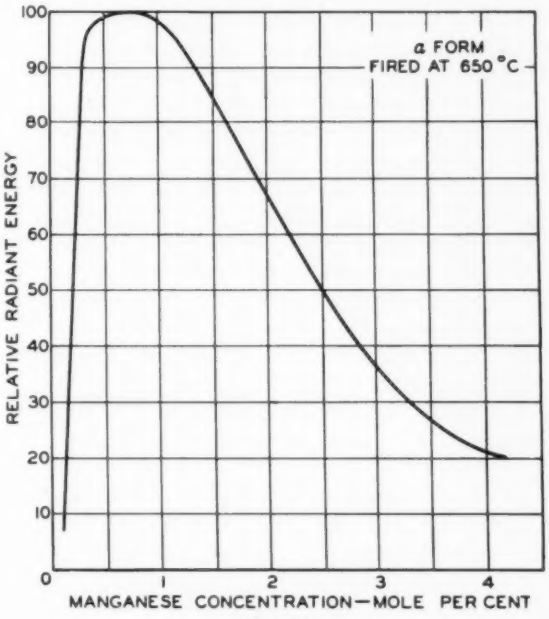

FIG. 2A

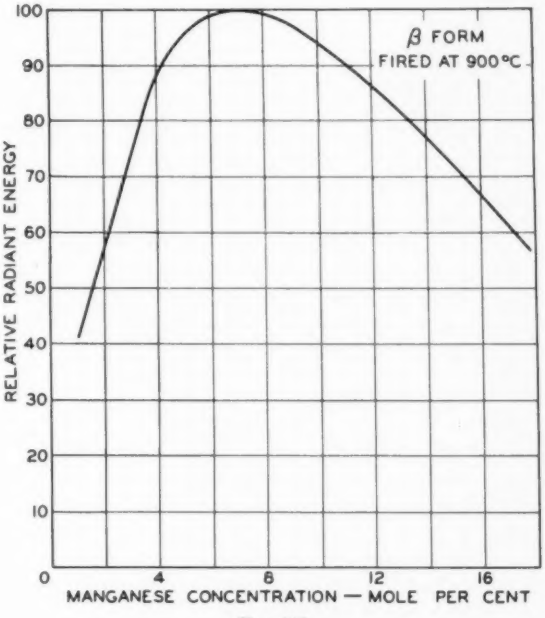

FIG. 2B

FIG. 2. Relative radiant energy at peak wavelengths

changed, although the emission will decrease in absolute intensity as a red band, due to the formation of the β form, makes its appearance (Fig. 2).

The conversion of the α to β form is complexly dependent on firing temperature and manganese concentration. If the manganese concentration is less than about 0.75 mole per cent, $Zn_3(PO_4)_2$:Mn may be fired at temperatures up to 1075°C and still retain the α form. If, however, the manganese concentration is raised above a value of about 1 mole per cent, then the phase change (and hence also the color of the emission) is a function of temperature. For example, with 1 mole per cent manganese (or more), firing at 700°C produces a pure α form emitting at 5520 Å. Temperatures between 700° and 800°C produce shades varying from yellow-green to orange-red. X-ray diffraction analyses of these powders showed that α and β forms were present together. Above 800°C only the β form is produced.

TABLE II. *Summary of data on luminescent characteristics*

Crystal form	Peak λ(Å)	Relative radiant energy at peak wavelength	Relative visible energy
		(approximate)	(approximate)
α	5520	40	100
β	6380	100	50
γ	6320	80	40

The cathodoluminescence of the pure β form is light red, the peak of the emission curve being at about 6380 Å (Fig. 1). Higher manganese concentrations have little effect on the shape of the curve or the wavelength at which peak emission occurs, although a slight shift of 20–30 Å toward the red is noticed as the concentration rises above 5 mole per cent. The efficiency, however, is lowered by increasing manganese content (Fig. 2*b*). The relative peak intensity of this form is more than double that of the α form (Table II).

Preparation of the γ Form

The third modification, or γ form, may be formed in a variety of ways, but the most positive is by the addition of 2 mole per cent (or greater) of magnesium orthophosphate. When less than 2 mole per cent of the magnesium compound is added with manganese present, a mixture of β and γ forms is produced, probably because the amount of magnesium is too small to be perfectly distributed. In the presence of magnesium, manganese plays no apparent part in the change to the γ phase of $Zn_3(PO_4)_2$, for it occurs both when no manganese is present and when it is present in very high proportions. Temperature is also not a critical factor, for with 5 mole per cent magnesium the transition to the γ form occurs at as low as 700°C.

Although the addition of magnesium gives what may be termed the purest γ form (in respect to simplicity and sharpness of its x-ray diffraction pattern), there are a variety of ways in which this phase may be produced. Zinc pyrophosphate additions to zinc orthophosphate in concentrations of 5 to 20 mole per cent give rise to the γ form. The conversion here is a function of temperature. At 700°C the α form is produced, while at approximately 800°C the conversion to the γ phase begins. This conversion is analogous to that from the α to the β form. The fact that the changes take place in the same temperature region leads to the supposition that the α form is stable to about 700°–750°C.

The γ phase is also produced, at least in part, by the addition of combinations of the following ions: Zn^{2+}, Mg^{2+}, O^{2-}, and Cl^-. Thus, addition of zinc chloride produces a β phase with a slight amount of the γ phase. Zinc oxide produces predominantly the γ phase, with some β phase also present. When oxides and chlorides of magnesium are added alone or in combination, x-ray diffraction patterns are obtained which resemble in general structure the pattern of both the γ phase and $Mg_3(PO_4)_2$ itself. It would appear that solid solutions occur, but it is difficult to say of what.

No new pattern corresponding to the Wagnerite type of compound (analogous to the apatite in form) can be distinguished. Mixtures designed to give $Zn_3(PO_4)_2 \cdot MO$ or $Zn_3(PO_4)_2 \cdot MCl_2$, where M is Mg or Zn, always showed basically a γ-form type diagram, although often quite distorted.

Discussion

Of particular practical import from the standpoint of obtaining consistent results with zinc orthophosphate phosphors is the prevention of contamination with double salts formed by zinc orthophosphate and alkali phosphates. Definite compounds of great stability having the generic form $ZnMPO_4$, where M is NH_4, Na, or Li, may be prepared either by precipitation or by solid-state reactions. Because of the relative insolubility of these compounds, great care must be exercised in precipitation to obtain a pure zinc orthophosphate free from alkali or ammonium ions. The reactions have already been discussed. If pyrophosphates are present in any great amount, the β form of the orthophosphate cannot be obtained, for pyrophosphate causes conversion to the γ form.

If sodium ions are present in the phosphor to any degree, several undesirable effects are produced. The main one is a shift toward shorter peak wavelengths, pure zinc sodium phosphate, $ZnNaPO_4$, having a

green-yellow emission with a peak at about 5450 Å. This compound melts at a comparatively low temperature, between 800°–850°C, so that even small amounts of residual sodium compounds cause severe sintering at these temperatures. [Although several publications (9, 10) give a melting point of 900°C for zinc orthophosphate, this value is definitely in error and was possibly obtained on samples containing sodium. A more probable value for the melting point is 1070°–1080°C.] Too, when sodium is present there is a tendency for increased phosphorescence, which is not desirable for some applications. Of major importance is a considerable drop in efficiency as the sodium concentration rises above 1 mole per cent.

Lithium is not usually encountered as an impurity, but some tests were conducted to determine the characteristics of $ZnLiPO_4$, since lithium salts were considered for use as fluxes. The compound $ZnLiPO_4$ has a yellow-orange emission which peaks at about 5650 Å and is of rather fair intensity. Additions of Li_3PO_4 to $Zn_3(PO_4)_2$ in amounts smaller than that necessary to form the definite compound $ZnLiPO_4$ cause a shift toward shorter wavelengths. Although x-ray diffraction tests have not been made, both the sodium and the lithium phosphates appear to be soluble in one of the forms of zinc phosphate, so that new base compounds are formed. The zinc phosphate-lithium phosphate system deserves further study, since both pure phosphates have only red emission, yet their double compound has an orange emission. The phenomena reported by Miller (6), yellow emission of "zinc orthophosphate" under infrared stimulation, was probably due to the inclusion of the lithium sulfate flux. Our investigations with double activation of zinc orthophosphate by Pb-Mn showed that only green emission was produced by infrared stimulation after excitation by 1850 Å radiation, regardless of whether the pyrophosphate concentration was zero or up to 20 mole per cent. The emission color was changed only by the addition of sodium or lithium ions to the matrix. These additions shifted the color toward longer wavelengths, giving yellow to orange emission (whether these were single or double bands was not determined). However, efficiencies for the yellow to orange emissions comparable to those obtained for the green could not be obtained; that is, the addition of sodium or lithium, while shifting the color, also lowered the efficiency. At best, the samples showed only a fraction of the stimulability of the alkaline-earth, rare-metal infrared sensitive phosphors.

It appears from the results obtained in this investigation that emissions in the orange to yellow range reported by some of the previous investigators were obtained on samples which (*a*) were contaminated by other products, such as pyrophosphate, alkali ions or the like, (*b*) were not fired to high enough temperatures, (*c*) contained intermediate concentrations of manganese, or (*d*) were affected by a combination of these conditions. Because of the paucity of preparative and optical data, it is impossible to state which of the possible red forms were prepared in the previous papers, since both red forms are so close in optical properties.

Of some theoretical interest is the position of the emission bands of the α and β forms. On the basis of the Linwood - Weyl - Schulman hypothesis (11, 12) concerning the role of the coordination position of manganese in relation to its emission, it may be predicted that the α form has manganese in fourfold coordination, since the emission is green. Since it is highly probable that manganese directly replaces zinc in the lattice, we may predict that the zinc in the α form is also of fourfold coordination. By analogous reasoning for the β and γ forms, it may be predicted that the transformation from the α form is one which the structure changes to a more compact arrangement of atoms with the zinc now being in sixfold coordination.

There is apparently little intersolubility of the α-β-γ forms, for x-ray diffraction analyses show no distortion in any of the patterns, regardless of the relative concentrations of the different forms in the sample. Too, the position of the emission bands is stable, showing no variation (except in intensity) with different proportions of α-β-γ forms present. Other compounds (such as magnesium oxide, magnesium phosphate, magnesium chloride, and zinc oxide) are, however, highly "soluble" in the γ form giving highly distorted x-ray diffraction patterns.

A considerable amount of experimental work remains to be done before this rather neglected system is completely defined. The difference in decay rates between the α and β forms, observed in the investigation but not quantitatively measured, merits further work. The rather noticeable change in decay rates within the same crystal form, dependent on preparative conditions, is worthy of more study from a practical, as well as from a theoretical, viewpoint.

Acknowledgments

The generous and often indispensable assistance of the following people is gratefully acknowledged: A. E. Hardy and R. F. Jefferies for measurements of efficiency and spectral distribution; J. A. Markoski, for advice and information on methods of precipitation of zinc orthophosphate; A. D. Power (RCA Harrison Laboratory) for the x-ray diffraction analy-

ses; and L. E. Whitmer for the preparation of samples.

Any discussion of this paper will appear in a Discussion Section, to be published in the June 1952 issue of the JOURNAL.

REFERENCES

1. L. LEVY AND D. W. WEST, *J. Inst. Elect. Engrs.* (*London*), **79,** 11 (1936).
2. S. T. HENDERSON, *Proc. Roy. Soc.* (*London*), **173,** 323 (1939).
3. E. IWASÉ, *Sci. Papers Inst. Phys. Chem. Research* (*Tokyo*), **38,** 67 (1946).
4. A. V. MOSKVIN, *Elektrichestvo,* **69** No. 3, 24 (1948).
5. F. A. KROEGER, "Some Aspects of the Luminescence of Solids," Elsevier Publishing Co., New York (1948).
6. N. F. MILLER, Final Report, "Infra-red Stimulation of Phosphors," P. B. Report No. 33363, Office of Technical Services, U. S. Dept. Commerce, Washington, D. C.
7. "Alphabetical and Grouped Numerical Index of X-Ray Diffraction Data," Special Technical Publication 48-B, American Society for Testing Materials, Philadelphia (1950).
8. A. E. HARDY, *Trans. Electrochem. Soc.*, **91,** 127 (1947).
9. N. A. LANGE, "Handbook of Chemistry," 7th ed., pp. 294–295, Handbook Publishers, Inc., Sandusky, Ohio (1949).
10. C. D. HODGMAN, Editor-in-chief, "Handbook of Chemistry and Physics," 32nd ed., pp. 598–599, Chemical Rubber Publishing Co., Cleveland, Ohio (1951).
11. S. H. LINWOOD AND W. A. WEYL, *J. Optical Soc. Am.*, **32,** 443 (1942).
12. J. H. SCHULMAN, *J. Applied Phys.*, **17,** 902 (1946).

Cathodoluminescence Characteristics of Some Barium-Zinc-Silicate Phosphors with Manganese Activator[1]

SIMON LARACH

Radio Corporation of America, RCA Laboratories Division, Princeton, New Jersey

ABSTRACT

Spectral distribution curves of cathode-ray-excited barium-zinc-silicate phosphors with manganese activator show the existence of blue, green, and red emission bands. The emission intensity of different bands was found to vary both with host crystal proportions and manganese content.

INTRODUCTION

Anderson and Wells have described some compositions in the barium-zinc-silicate system, using mainly 2537 Å radiation as the exciting source (1). Their finding that barium-zinc silicates respond to cathode rays, giving a red fluorescence, led to further investigations of this system. Accordingly, various compositions were prepared and tested under cathode rays. The present paper reports the results found with various ratios of $BaO:ZnO:SiO_2$ and different manganese proportions. Many differences were noted between the previously reported (1) u.v.-excited and the present c.r.-excited measurements.

PREPARATION OF PHOSPHORS

The chemicals used in the preparation of the phosphors consisted of C.P. grade BaO_2, A.R. grade ZnO, and a special bulky silica of 9.0 per cent water content. The various compositions were dry milled for four hours in order to insure complete mixing; manganese, as $MnCl_2$ solution, was added; the mixture was slurried with triple-distilled water, dried at 150°C, transferred to a silica boat, and fired in a tube furnace. All subsequent designations of manganese content are given as weight per cent of Mn.

Fig. 1 is a composition diagram of the system $BaO:ZnO:SiO_2$. The points indicate the various compositions tried.

RESULTS

$BaO \cdot 2ZnO \cdot 2SiO_2$:Mn(0.5), fired at 1100°C in air, showed a double band emission under c.r. excitation. This is shown in Fig. 2. Whereas Anderson and Wells found the green peak to be of much lesser intensity than the red peak, the reverse is found with c.r. excitation. This may be caused by the higher energy particles exciting the shorter wavelength band more than the longer wavelength band.

[1]Manuscript received April 24, 1951. This paper prepared for delivery before the Philadelphia Meeting, May 4 to 8, 1952.

The effect of variations of manganese content on the light output at 5300 and 6900 Å in $BaO \cdot 2ZnO \cdot 2SiO_2$:Mn($x$) is shown in Fig. 3. It is seen that increasing manganese from 0.5 to 5.0 per cent resulted

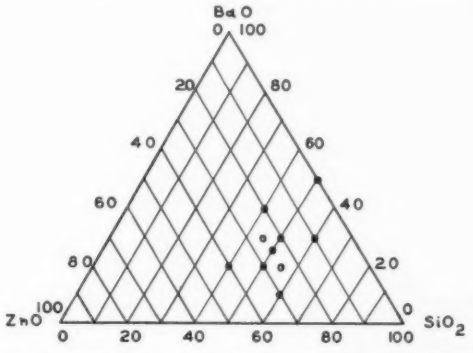

FIG. 1. Compositions tested in the system $BaO:ZnO:SiO_2$

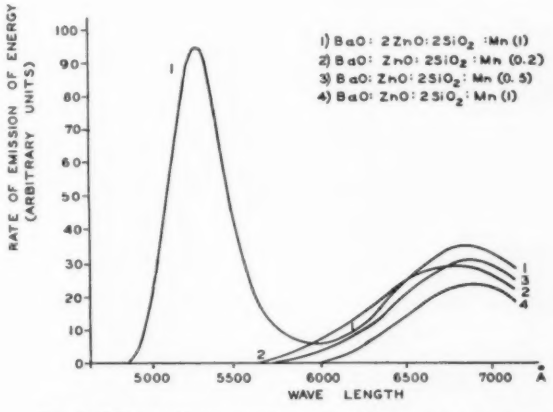

FIG. 2. Effects of host crystal composition and manganese content on spectral distribution (c.r. excitation).

in a linear decrease of output at 6900 Å, while an optimum at 1 per cent manganese was found for the output at 5300 Å.

Although Anderson and Wells state that only one ratio of BaO to ZnO was effective as a red photo-

luminescent material, namely 1 BaO to 2 ZnO, it was found that under c.r. excitation a ratio of 1 BaO to 1 ZnO, i.e., $BaO \cdot ZnO \cdot 2SiO_2$:Mn, resulted in a single band red emission, with no trace of the green (5300 Å) band. Increase of manganese content was found to shift the feet of the curve toward longer wavelengths, so that 0.2 per cent Mn gave an orange-red emission, while 0.5 per cent gave red, and 2 per cent gave a very deep red. The spectral distribution curves of these materials are shown in

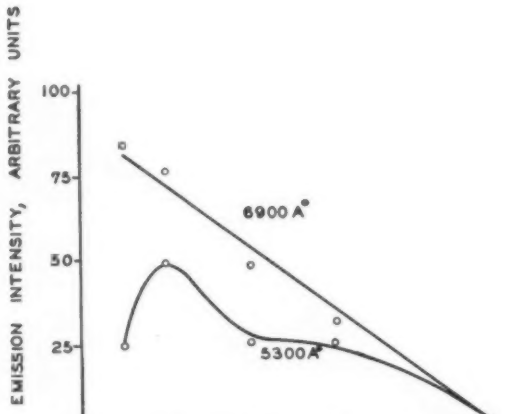

FIG. 3. Effect of manganese content on the emission intensities of the 5300 Å and 6900 Å bands of $BaO \cdot 2ZnO \cdot 2SiO_2$:Mn (c.r. excitation).

TABLE I. *Compositions and peak wavelengths of some barium-zinc-silicate phosphors with manganese activator*

Composition	Cathode-ray emission, peak wavelengths, Å
$2BaO \cdot ZnO \cdot 2SiO_2$	5300
$3BaO \cdot ZnO \cdot 6SiO_2$	4400
$BaO \cdot 3ZnO \cdot 6SiO_2$	6900
$3BaO \cdot 2.5ZnO \cdot 4.5SiO_2$	5300, 6900
$3BaO \cdot 2ZnO \cdot 5SiO_2$	5300, 6900
$2BaO \cdot 3ZnO \cdot 5SiO_2$	5300, 6900
$2BaO \cdot 2.5ZnO \cdot 5.5SiO_2$	5300, 6900

Fig. 2. These curves were obtained with an automatic, recording spectroradiometer (2) and a special demountable cathode-ray tube operating at 6 kv and a current density of approximately 1 $\mu a/cm^2$.

Further changes in host crystal composition and the resulting emission peak wavelengths are given in Table I, where the underlined wavelength indicates the more intense band. It was found that $2BaO \cdot ZnO \cdot 2SiO_2$:Mn(0.5) had a single green emission band, whereas $3BaO \cdot ZnO \cdot 6SiO_2$:Mn(0.5) had a weak blue emission, with peak wavelength approximately 4400 Å.

In systems of complex emission bands, the more persistent phosphorescence emission is usually that of the longer wavelength (3). However, it was observed that in the case of several of the BaZn-silicate:Mn phosphors, having both green and red bands, the phosphorescence emission was green. It is possible that some of the products may be heterogeneous, perhaps with the formation of a separate phase of green-emitting Zn_2SiO_4:Mn to account for the intense green emission band. X-ray diffraction patterns proved extremely complex and were not readily interpretable in terms of the luminescences observed. For example, the green- and red-emitting $2BaO \cdot 2.5ZnO \cdot 5.5SiO_2$:Mn showed only the patterns of red-emitting $BaO \cdot ZnO \cdot 2SiO_2$:Mn and of zinc oxide.

Under c.r. excitation, $BaO \cdot 2ZnO \cdot 2SiO_2$:Mn and $BaO \cdot ZnO \cdot 2SiO_2$:Mn had approximately 15 per cent more output at 6900 Å than Cd-borate:Mn. At 6215 Å, the peak wavelength for Cd-borate:Mn, the barium-zinc-silicate output was 18 per cent that of the borate.

In confirmation of Iwasé (4), it was found that the cathodoluminescence of barium silicate with manganese activator was blue.

Conclusions

Cathode-ray excitation of barium zinc silicate phosphors with manganese activator yields complex spectra involving single band blue, green, and red, as well as double band green- and red-emitting materials. Unlike the results found with ultraviolet excitation, the c.r.-excited emission spectrum was found to be a function of both host crystal composition and manganese content.

Acknowledgments

The author wishes to acknowledge the assistance of Drs. R. H. Bube and R. E. Shrader in measurements of spectral distributions, and of Mr. I. J. Hegyi for the x-ray diffraction measurements.

Any discussion of this paper will appear in a Discussion Section, to be published in the June 1952 issue of the JOURNAL.

REFERENCES

1. J. T. Anderson and R. S. Wells, *J.* (*and Trans.*) *Electrochem. Soc.*, **95**, 299 (1949).
2. V. K. Zworykin, et al., *J. Optical Soc. Am.*, **29**, 84 (1939).
3. H. W. Leverenz, "Introduction to Luminescence of Solids," p. 256, John Wiley & Sons, Inc., New York (1950).
4. E. Iwasé, *Sci. Papers Inst. Phys. Chem. Research* (*Tokyo*), **38**, 76 (1940).

The Thermoluminescence Characteristics of Silicate Phosphors Activated by Manganese and Arsenic[1]

C. Bull and G. F. J. Garlick

Physics Department, University of Birmingham, England

ABSTRACT

A quantitative investigation has been made of the effect of inclusions of arsenic on the thermoluminescence characteristics of various manganese-activated silicate phosphors. It is found that the complex distributions of the thermal activation energies of the electron trapping states in Zn_2SiO_4-Mn, $(Zn, Be)_2SiO_4$-Mn, $CdSiO_3$-Mn, and $(Zn, Cd)_2SiO_4$-Mn phosphors are greatly modified by small inclusions (1 in 10^5) of arsenic, and that in all cases the total number of electron traps is greatly increased. Other silicate systems, notably $SrSiO_3$-Mn, $BaSiO_3$-Mn, and $CaSiO_3$-Mn, do not show this effect.

Introduction

The phosphorescence decay of manganese-activated zinc silicate phosphors at room temperature consists of two components (1). The initial decay is exponential and is followed after about 30 milliseconds by a relatively weak phosphorescence which is due to the presence of electron trapping states (2). Froelich and Fonda (3) have shown that this phosphorescence can be considerably enhanced by including small amounts of arsenic in the phosphor. The persistence of the phosphorescence increased with arsenic content, for concentrations up to 0.5 per cent, but the fluorescence intensity at room temperature decreased slightly as the arsenic concentration increased. Similar, but much less pronounced, effects were observed on including arsenic in manganese-activated cadmium silicates and zinc-beryllium silicates. Unfortunately, these phosphorescence decay measurements were made only at room temperature, so that little information about the trapping states responsible for the phosphorescence can be obtained. In the following studies the thermoluminescence experiment has been used to determine the effect of arsenic inclusions on the electron trapping states of various silicate phosphors.

Experimental Methods

Techniques previously developed in this laboratory have been used to study the thermoluminescence properties of these phosphors. The phosphors, mounted as very thin layers on a surface in vacuo, were excited by the focused radiation from a 125-w high pressure mercury arc with quartz envelope, using a Corning 986 filter to select short wavelength ultraviolet radiation. Phosphors not excited by such irradiation were subjected to a high frequency discharge produced in the residual gas of the vacuum apparatus containing the phosphor. After excitation at 90°K the phosphor was warmed and the variation of the thermoluminescence intensity with temperature (the "thermal glow curve") was measured. Previous studies have shown that the release of electrons from traps of thermal depth E gives rise to thermoluminescence at a temperature T_G (the "glow temperature") which is approximately proportional to E. For the silicate phosphors considered, the relationship is $T_G \simeq 500\ E$. The heating rate used was 3°K per second. This was constant over the range 100°–500°K so that relative light sums could be calculated by measuring the areas under thermal glow curves. After the experiment the specimen was weighed so that an estimate of the relative number of trapping states in different specimens was possible by comparison of the thermal light sums per unit weight of phosphor.

The emission intensity of the phosphor was measured by focusing the radiation onto the cathode of a RCA 931A photomultiplier; the output current was measured with a d'Arsonval galvanometer and manually operated pen recorder.

All the silicate phosphors were prepared by heating in open silica tubes in a closed muffle gas furnace.

Experimental Results

Arsenic-Activated and Pure Zinc Silicate Phosphors

Specimens of zinc silicate, without deliberate impurity inclusions, prepared by firing at 1200°C showed a feeble blue fluorescence when excited by short wavelength ultraviolet radiation. This observation agrees with those of Leverenz and Seitz (4), but conflicts with those of Kroeger (5) and Randall (6), in which no fluorescence was found. The thermoluminescence characteristics of all specimens were very similar; a typical thermal glow curve is given in curve *a* of Fig. 1.

[1] Manuscript received February 27, 1951. This paper prepared for delivery before the Washington Meeting, April 8 to 12, 1951.

When small amounts of arsenic are included during preparation, the fluorescence becomes green, and the thermoluminescence is considerably enhanced. The maximum thermal light sum is obtained with specimens containing 0.04 per cent of arsenic in the pentavalent form, the light sum then being about 40 times that of the unactivated phosphor. The thermal glow curves of phosphors containing pentavalent arsenic consist of four sharp peaks as shown in curve *b* of Fig. 1. The half-widths of these peaks are approximately 46°K, 43°K, 56°K, and 57°K, compared with calculated half-widths of 30°K, 41°K, 51°K, and 57°K for thermal glow peaks at the same temperatures due to groups of electron traps each having a single activation energy. [These are calculated from the theory of Randall and Wilkins (2), assuming a value for their constant, s, of $1.5 \cdot 10^9$ sec^{-1}, as determined by Garlick and Gibson (7)]. This agreement shows that well-defined groups of trapping states are produced by the pentavalent arsenic inclusions.

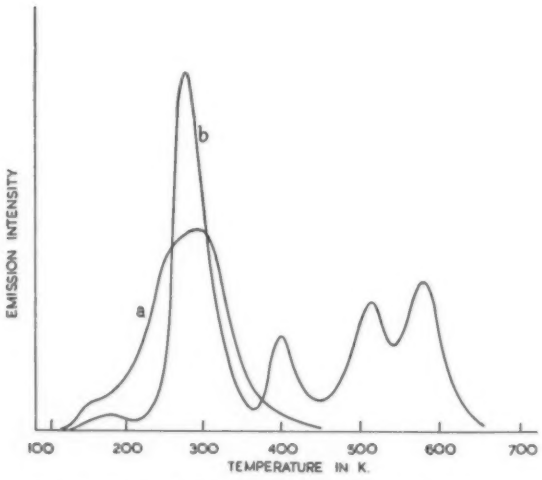

FIG. 1. Thermal glow curves of: (*a*) pure Zn_2SiO_4 phosphor; (*b*) Zn_2SiO_4-As (0.02%) phosphor.

The thermoluminescence characteristics of these phosphors were not appreciably affected by the presence of excess silica of up to 1 mole concentration.

When arsenic in the trivalent form was added during preparation the fluorescence was much less intense and the thermal light sums were much smaller than when pentavalent arsenic was used. The thermal glow curve showed only one peak, at 280°K with a broad continuum extending from 440°K to above 600°K. This result is at variance with that obtained by Froelich and Fonda (3).

In the phosphors described in the following sections the arsenic inclusions were always in the pentavalent state.

Manganese- and Manganese-Arsenic-Activated Zinc Silicate Phosphors

Manganese-activated zinc silicate phosphors, produced as described above, are strongly green fluorescent and have a complex thermal glow curve, as shown in Fig. 2. The form of the latter varies little with the manganese content. The maximum thermal light sum is obtained with a manganese concentration of 0.3 per cent, in general agreement with previous results.

When arsenic and manganese are included as impurities the total number of electron traps is greatly increased, and the complex thermal glow curve due to either activator is replaced by a single thermal glow peak, as shown in Fig. 2. This has a peak at

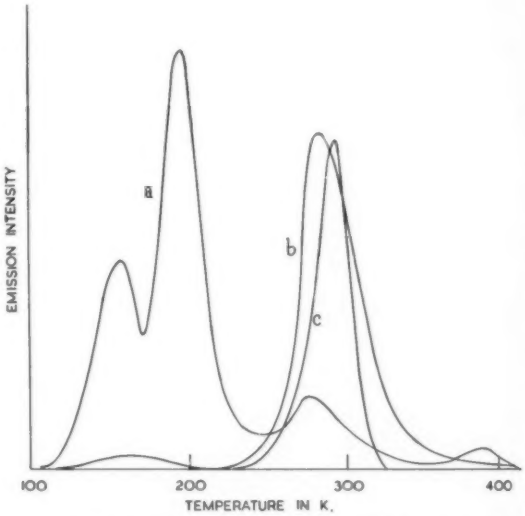

FIG. 2. Thermal glow curves of: (*a*) Zn_2SiO_4-Mn (0.04%) phosphor; (*b*) Zn_2SiO_4-Mn(0.2%)-As (0.01%) phosphor; (*c*) theoretical curve—$E = 0.6$eV, $s = 1.5 \cdot 10^9/sec^{-1}$.

285°K and a half-width of about 45°K, compared with a theoretical half-width of 30°K for a peak at this temperature due to electron traps of a single depth (7). One of the thermal glow peaks of Zn_2SiO_4-As occurs at almost the same temperature.

The shape of the thermal glow curve is independent of the manganese and arsenic concentrations over wide ranges, although the relative number of trapping states, as determined from the thermal light sums, is strongly dependent on these concentrations. All the members of a series of Zn_2SiO_4-Mn (0.32%) phosphors containing between 0.0003 and 1.3 per cent of arsenic show the single peak glow curve, the form of which is almost independent of the arsenic content. With an arsenic concentration of 0.017 per cent the thermal glow curve of all phosphors containing between 0.05 and 2 per cent man-

ganese consists of the single sharp peak. The shape of the glow curve is unaffected by the presence of excess ZnO or SiO_2, up to 1 mole of either. The number of trapping states and the fluorescence intensity are, however, greatly reduced when excess ZnO is present.

The variation of the number of electron traps with the arsenic concentration in two series of zinc silicate phosphors, with differing manganese contents, is shown in Fig. 3. It is seen that the maximum number is in both cases about 50 times that found in similar Zn_2SiO_4-Mn phosphors containing no arsenic, and that the maximum number occurs when the manganese concentration is approximately 100 times the arsenic concentration.

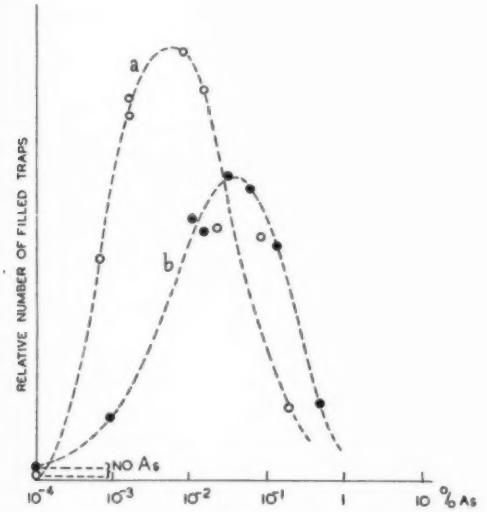

FIG. 3. The variation of the number of trapping states with arsenic concentration in: (*a*) Zn_2SiO_4-Mn (0.32%) phosphors; (*b*) Zn_2SiO_4-Mn (1.9%) phosphors.

Zinc-Beryllium Silicates

Kroeger (8) has shown that Zn_2SiO_4, Be_2SiO_4, and Mn_2SiO_4 form a ternary mixed system possessing the willemite structure for Be_2SiO_4 concentrations up to about 10 mole per cent. The fluorescence of (Zn, Be)$_2SiO_4$-Mn phosphors is green with small beryllium inclusions, but becomes progressively more yellow as the beryllium concentration is increased. Schulman (9) has shown that this color change is due to the appearance of a new emission band with a maximum at 6000 Å.

Similar experiments to those described in the last section were made on several series of phosphors containing varying amounts of manganese, arsenic, and beryllium. The thermal glow curves of unactivated (Zn, Be)$_2SiO_4$ phosphors and of those containing manganese or arsenic alone are complex (Fig. 4), but phosphors containing manganese and arsenic show a more simple thermal glow curve. This consists of a broadened peak, due to the superposition of two separate peaks, having maxima at 285° and 320°K. The relative heights of the two peaks vary

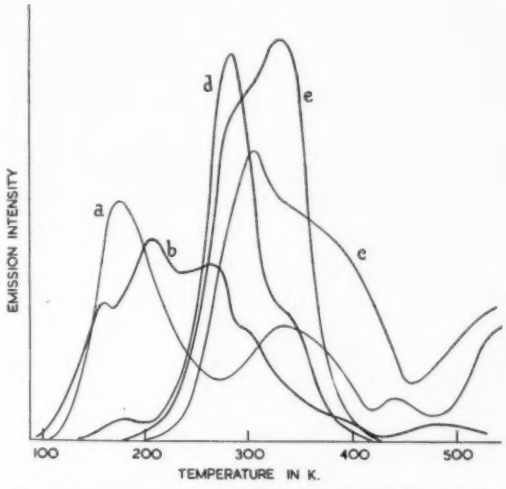

FIG. 4. Thermal glow curves of: (*a*) (92% Zn, 8% Be)$_2$-SiO_4 phosphor; (*b*) (92% Zn, 8% Be)$_2SiO_4$-Mn (0.2%) phosphor; (*c*) (92% Zn, 8% Be)$_2SiO_4$-As (0.01%) phosphor; (*d*) (95% Zn, 5% Be)$_2SiO_4$-Mn (0.2%)-As (0.003%) phosphor; (*e*) (95% Zn, 5% Be)$_2SiO_4$-Mn (0.2%)-As (0.2%) phosphor.

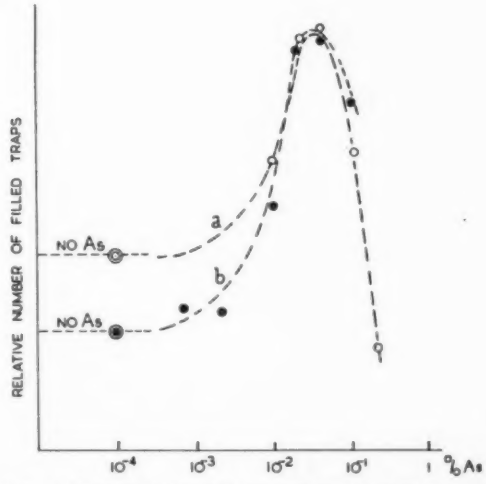

FIG. 5. The variation of the number of trapping states with arsenic concentration in: (*a*) (95% Zn, 5% Be)$_2SiO_4$-Mn (0.18%) phosphors; (*b*) (92% Zn, 8% Be)$_2SiO_4$-Mn (0.2%) phosphors.

with the beryllium content, the 320°K peak being more prominent at high concentrations, and apparently also with the arsenic concentration, as shown in Fig. 4.

The total number of trapping states varied with the arsenic concentration in a manner similar to

that observed for Zn_2SiO_4-Mn-As phosphors. This variation is shown in Fig. 5 for two series of (Zn, Be)$_2SiO_4$-Mn phosphors.

Zinc-Cadmium Silicates

The normal form of cadmium silicate is $CdSiO_3$, but the orthosilicate, Cd_2SiO_4, is formed in a mixed

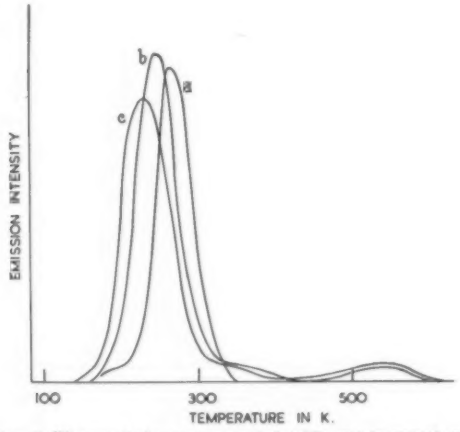

FIG. 6. Thermal glow curves of: (*a*) (Zn,Cd (0.26%))$_2SiO_4$-Mn (0.2%)-As (0.02%); (*b*) (Zn,Cd (6.7%))$_2$ SiO_4-Mn (0.2%)-As (0.02%); (*c*) (Zn,Cd (13%))$_2$ SiO_4-Mn (0.2%)-As (0.02%).

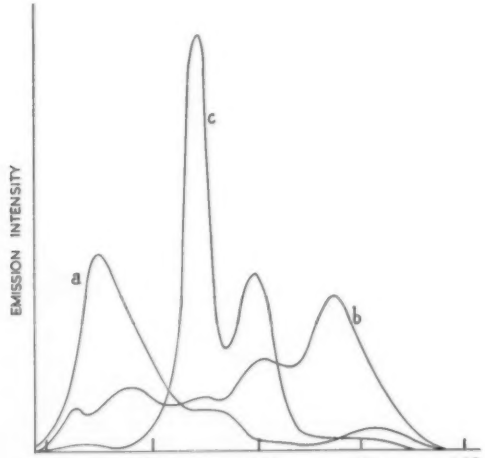

FIG. 7. Thermal glow curves of: (*a*) $CdSiO_3$-As (0.1%); (*b*) $CdSiO_3$-Mn (0.17%); (*c*) $CdSiO_3$-Mn (0.17%)-As (0.1%).

zinc silicate-cadmium silicate system. According to Kroeger (8) the solubility limit is 20 mole per cent Cd_2SiO_4.

Similar phenomena to those described above were observed when manganese and arsenic were included in (Zn, Cd)$_2SiO_4$. The thermal glow curve of such phosphors consists of a single narrow peak, but the temperature of the maximum of this peak depends on the cadmium content, varying from 285°K with (87% Zn, 13% Cd)$_2SiO_4$-Mn-As, as shown in Fig. 6. A further increase in the cadmium content has little effect on the position of the thermal glow peak.

Cadmium Silicates

Pure cadmium silicate is only feebly fluorescent under short wavelength ultraviolet irradiation. Specimens activated by manganese show a strong orange fluorescence, while those activated by arsenic show a yellow fluorescence. Typical glow curves of such phosphors are given in Fig. 7.

When both activators are included the thermal glow curve is considerably altered and consists of two sharp peaks having maxima at 250° and 305°K (Fig. 7). Variations in the arsenic content between 0.01 and 0.4 per cent and in the manganese content between 0.10 and 4 per cent have no effect on the

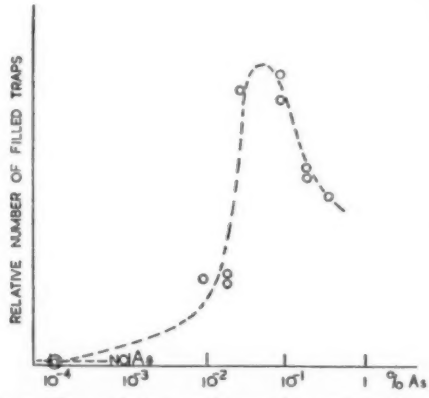

FIG. 8. The variation of the number of trapping states with arsenic content in $CdSiO_3$-Mn (0.17%) phosphors.

positions of these peaks, but the relative heights of the two peaks vary from specimen to specimen in a manner not apparently associated with the manganese or arsenic concentrations. In general the thermal light sum due to the shallower traps is about twice that due to the deeper ones. The variation of the total number of trapping states with arsenic concentration for a series of phosphors containing 0.17 per cent manganese is shown in Fig. 8. The maximum number is about 50 times that occurring in $CdSiO_3$-Mn, and occurs for an arsenic concentration of about 0.1 per cent.

Other Silicate Systems

Other silicate phosphors have been examined for phenomena similar to those described above. Calcium silicate phosphors activated by manganese are not excited by 2537 Å radiation unless lead is also present as a sensitizer. The nonsensitized phosphors are, however, strongly fluorescent under cathode ray bombardment, or when in a gaseous discharge. It was found, however, that in neither the sensitized

nor the nonsensitized $CaSiO_3$-Mn phosphors do arsenic inclusions have any effect on the number of the electron traps or the distribution of their thermal activation energies.

Similarly, arsenic inclusions do not appear to have any effect on the thermoluminescence of $BaSiO_3$-Mn, $SrSiO_3$-Mn, or $MgSiO_3$-Mn phosphors.

Discussion of Results

The results given above clearly show that arsenic has a pronounced effect on the trapping states responsible for phosphorescence and thermoluminescence in manganese-activated zinc, zinc-beryllium, zinc-cadmium, and cadmium silicate phosphors. The measurement of thermal glow curves has provided more information about the modifications of the trap distributions produced by arsenic inclusions than can be obtained by measurements of phosphorescence decay at one fixed temperature. Several points for discussion arise from these and previous results, and may be summarized as follows:

1. Arsenic produces a much more marked effect on trapping states when included in the phosphor in the pentavalent form than when in the trivalent form.

2. Arsenic inclusions have little or no effect on manganese - activated calcium, strontium, barium, and magnesium silicate phosphors.

3. The largest number of electron trapping states in zinc, zinc-beryllium, and zinc-cadmium silicate phosphors occurs when the arsenic concentration is approximately 1 per cent of the manganese concentration. In cadmium silicate it occurs when the arsenic and manganese concentrations are about equal.

4. The maximum number of trapping states produced in the above phosphor systems by arsenic inclusions is about 50 times that produced by the manganese impurity alone.

5. The thermal glow curves of phosphors containing manganese and arsenic are simple in form, indicating that a very specific type of trapping state is produced.

It is also of interest to note that although large numbers of electron traps exist in zinc silicate phosphors activated by manganese and arsenic, no dielectric effects of the type found in zinc sulfide phosphors are observed when the phosphors are excited. The phosphors show photoconductivity, but this is characteristic of the pure silicate and is not appreciably affected by the presence of manganese or arsenic.

Schulman (9) has put forward a tentative explanation of the action of As^{5+} ions in the silicate phosphors. He suggests that because of their similar radii these ions can replace Si^{4+} ions in the lattice, their excess positive charge constituting an immobile positive hole capable of trapping an electron. Such a mechanism would result in a single peak thermal glow curve. However, the thermal glow curves of arsenic-activated zinc silicate phosphors show four peaks, the single peak glow curve being observed only when manganese is also present. It must also be remembered that when the substitution of a pentavalent ion into a quadrivalent lattice point is attempted, the diameter of the pentavalent ion will probably be modified by the coulomb forces acting on it.

The centers producing these singular trapping states are complex, probably involving many manganese and arsenic ions as well as those of the host lattice.

The two peaks in the thermal glow curves of zinc-beryllium silicates containing manganese and arsenic may be associated with the Zn_2SiO_4 and Be_2SiO_4 groups in the lattice, since one of these peaks occurs at the same temperature as that in Zn_2SiO_4. However, a different effect is observed with mixed zinc silicate-cadmium silicate phosphors activated with manganese and arsenic, the single peak glow curve being observed in all the cases. The decrease in the thermal activation energy of the trapping states as the cadmium content is increased is possibly due to a progressive change in the lattice parameters.

Since the singular trapping state due to arsenic is also observed in $CdSiO_3$ phosphors, it would appear that the orthosilicate form is not necessary for its production. However, $CdSiO_3$ phosphors may contain a small concentration of orthosilicate type groups not detectable by x-ray analysis. The non-appearance of the effect in alkaline earth silicates might thus be attributed to the different coordination of silicate groups in these materials.

Single crystals of zinc silicates of considerable size have already been made, and if it is possible to incorporate manganese and arsenic impurities into these, further valuable information about their sites might be obtained from a study of their infrared absorption characteristics.

Any discussion of this paper will appear in a Discussion Section, to be published in the June 1952 issue of the Journal.

REFERENCES

1. G. R. Fonda, *J. Applied Phys.*, **10,** 408 (1939).
2. J. T. Randall and M. H. F. Wilkins, *Proc. Roy. Soc. (London)*, **A184,** 347, 366 (1945).
3. H. C. Froelich and G. R. Fonda, *J. Phys. Chem.*, **46,** 878 (1942).
4. H. W. Leverenz and F. Seitz, *J Applied Phys.*, **10,** 479 (1939).
5. F. A. Kroeger, *Physica*, **6,** 764 (1939).
6. J. T. Randall, *Nature*, **142,** 113 (1938).
7. G. F. J. Garlick and A. F. Gibson, *Proc. Phys. Soc. (London)*, **A188,** 485 (1948).
8. F. A. Kroeger, "Luminescence in Solids Containing Manganese," Van Campen, Amsterdam (1940).
9. J. H. Schulman, *J. Applied Phys.*, **17,** 902 (1946).

The Effect of Temperature on Emission of Fluorescent Lamp Phosphors[1]

CHARLES W. JEROME

Sylvania Electric Products Inc., Salem, Massachusetts

ABSTRACT

The effect of temperature on over-all emission of phosphors as predicted by the theory developed by Kroeger satisfactorily explains the effects found in the present study. This theory leads to reasonable values of excitation energies.

The effect of temperature on the band width of the emissions is satisfactorily explained on the basis of the potential energy curve theory advocated by Butler. It has been shown that this effect over a narrow temperature range can be approximated by an assumed simplified shape of the potential energy curve, but that when a wide range of temperatures is used such approximations lead to inaccurate results.

INTRODUCTION

In a recent paper (1) Butler developed an explanation for the existence of emission bands having a Gaussian distribution of energy with frequency in phosphors activated by manganese or lead, or a combination of the two. He also discussed, on the basis of this and other theories, the effect which temperature should have on the emission bands. Since the effect of temperature on the emission of these phosphors is capable of experimental determination, the present study was undertaken in part to test the validity of the theories discussed.

EXPERIMENTAL PROCEDURE

These experiments are divided into two categories: (*a*) the effect of temperature on the intensity of emission of phosphors in air, and (*b*) the effect of temperature on the spectral energy distribution of these phosphors in fluorescent lamps.

The equipment used in making the measurements in the first category is shown in Fig. 1.

A shallow circular depression was milled in the surface of an electrically controlled hotplate *A*. The phosphor to be examined was packed into this depression in a solid thin layer *B*. A thermocouple *C* imbedded in the surface of the hotplate at the edge of the phosphor layer measured the temperature. The phosphor was irradiated by two U-shaped 4-watt germicidal lamps *D* and the output of the phosphor was measured with a photoelectric cell *E*. Readings of the photocell with an inert white powder in place of the phosphor were taken and subtracted from the phosphor readings to eliminate the contribution of the visible light emitted by the ultraviolet (u.v.) lamps.

[1] Manuscript received March 26, 1951. This paper prepared for delivery before the Washington Meeting, April 8 to 12, 1951.

It was found that the housing containing the u.v. lamps and photocell could be left over the hotplate only when readings were being made, since the heat from the plate affected the u.v. output of the lamps. Therefore, this housing was kept separate except for the few seconds required to make a reading, and the u.v. output was kept constant by monitoring with a u.v. meter prior to each reading. The lamps were further protected from the heat of the hotplate by a layer of u.v. transmitting glass *F*.

The heating element of the hotplate was controlled by a rheostat and temperature varied by small increments in the setting. The hotplate was allowed to come to temperature equilibrium at each new setting and maintained constant by the rheostat setting for two minutes. The u.v. output of the lamps was then brought to a standard reading on the u.v. meter by its separate electrical control after which the housing was placed over the hotplate and the reading of the photocell determined on a microammeter. The housing was then removed, a new setting made on the hotplate control, and the process repeated until the full range of temperatures desired had been covered. The emissions of the following phosphors were tested by this method: magnesium tungstate, barium silicate (Pb), zinc beryllium silicate (Mn), and calcium halophosphate (Mn, Sb). Calcium silicate (Pb, Mn) was also tested but was found to be very insensitive to heat and to show no appreciable decrease in emission up to 300°C.

The effect of temperature on the spectral energy distribution of the phosphors was determined with the powders in 40 T 12 fluorescent lamps. A small box enclosed a central 8-in. portion of the lamp and the temperature inside the box was regulated by a stream of air passed through a heater, as shown in Fig. 2. A thermocouple cemented to the bulb wall measured the temperature of the glass. Since the

glass wall is thin and the layer of phosphor is also thin and in contact with the glass, it is assumed that the temperatures of the glass and phosphor are essentially the same. Light from the lamp inside the box enters the entrance slit of a spectroradiometer (2) through a 4-in. glass window. The absorption of this window was determined and was found to have no appreciable spectral selectivity. Therefore, no correction was deemed necessary for the radiometric curves and those shown herein are just as determined on the spectroradiometer.

The small box enclosing and heating only a small portion of the lamp was necessary in order to separate the effects of temperature on the phosphor and

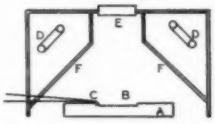

FIG. 1. Apparatus for measuring heat sensitivity of phosphors. A—Electrically controlled hotplate, B—shallow depression for phosphor, C—thermocouple, D—G4T4 germicidal lamps, E—photoelectric cell, F—u.v. transmitting glass.

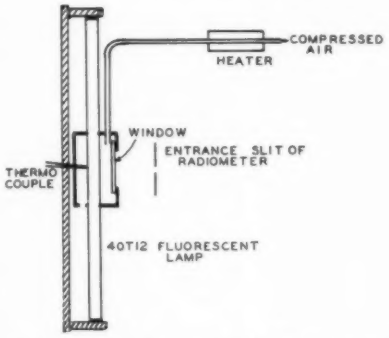

FIG. 2. Apparatus for measuring heat sensitivity of phosphors in lamps.

its effect on the electrical characteristics of the lamp. When the whole lamp is enclosed the heat increases the pressure in the lamp with the result that a much greater decrease in emission is obtained than can be attributed to the decreased emission of the phosphor alone. In one case where the whole lamp was enclosed, a temperature of approximately 175°C increased the pressure in the lamp to a point where the arc could no longer be maintained. Heating the whole lamp, however, more nearly approximates actual operating conditions at elevated temperatures such as for fluorescent lamps in fully enclosed fixtures. As will be indicated in the results discussed below, heating only a small portion of the lamp affects the operating characteristics slightly, but enough to yield spurious results of the temperature dependence of efficiency. However, these experiments lead to valid shapes of the spectral energy distribution curves.

Temperatures below room temperature were also investigated by replacing the air heater with a chamber filled with dry ice. However, in this experiment, as in that in which the whole lamp is enclosed and heated, the effect on the operating characteristics of the lamp is greater than the effect on the phosphor. In this case, the cooled portion of the lamp acts as a trap for the mercury vapor, effectively eliminating it from the arc stream. This results in reduced u.v. radiation to activate the phosphor.

THEORY

Kroeger (3) has shown that the efficiency of a phosphor is given by

$$\eta = p \frac{K_f}{K_f + K_d} \qquad \text{(I)}$$

where p is the fraction of the exciting energy actually absorbed by the activator, K_f is the probability of the fluorescent transition, and K_d that of a dissipation process. According to Mott (4) and Seitz (5), the probability of a radiationless dissipation of energy increases with rising temperature according to the formula:

$$K_d = C \exp(-\epsilon/kT) \qquad \text{(II)}$$

where ϵ is the activation energy, k is Boltzmann's constant, T is the absolute temperature, and C is a constant. Therefore, assuming that p and K_f are constants with respect to temperature, an assumption which Kroeger's work has indicated to be valid, equation (I) can be written:

$$\eta/p = P = A/[A + B \exp(-\epsilon/kT)] \qquad \text{(III)}$$

where A and B are constants.

Rearranging equation (III):

$$(1-P)/P = B/A \exp(-\epsilon/kT). \qquad \text{(IV)}$$

Taking logs of both sides:

$$\log \frac{1-P}{P} = -\frac{\epsilon}{2.3\,kT} + \log \frac{B}{A}. \qquad \text{(V)}$$

Therefore, plotting $\log (1-P)/P$ against $1/T$ should yield a straight line of slope $-\epsilon/2.3k$. From this slope, then, the activation energies of the phosphors can be calculated for the transition from a radiating state to a radiationless state.

Butler (1) has shown that the existence of Gaussian emission bands in phosphors can be explained on the basis of the potential energy curves of the normal and excited states of the activator. He also points out that the width of the emission band in-

creases with temperature by an equation which is roughly:

$$\sigma = a(b + T)^{\frac{1}{2}}. \qquad \text{(VI)}$$

That is, σ^2 is a straight line function of T. This is based on the approximation that the potential energy curves have a parabolic shape. As will appear later, this approximation is satisfactory over a limited range of temperatures, but over wide ranges a more exact formula for the shape of the potential energy curve must be employed.

For zinc-beryllium silicate $\log 1-P/P = -1440\ 1/T + 2.695$ (VIII)

For barium silicate $\log 1-P/P = -943\ 1/T + 1.960$ (IX)

For calcium halophosphate

(*a*) Over-all emission $\log 1-P/P = -1550\ 1/T + 2.551$ (X*a*)

(*b*) Antimony band $\log 1-P/P = -2150\ 1/T + 3.613$ (X*b*)

(*c*) Manganese band $\log 1-P/P = -1439\ 1/T + 2.259$ (X*c*)

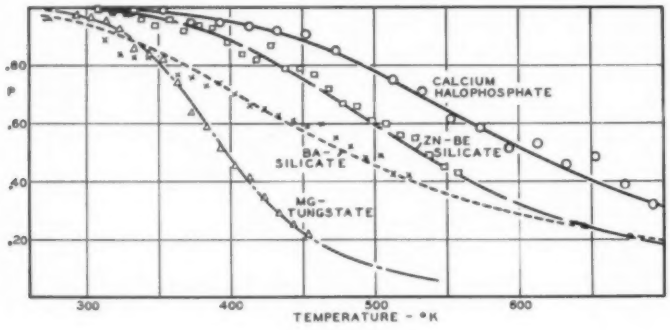

FIG. 3. Temperature sensitivity of lamp phosphors (P vs. T).

EFFICIENCY VS. TEMPERATURE

The relative efficiencies P of the several phosphors measured in air as described above were expressed as percentages of the value at room temperature and are shown plotted in Fig. 3. Log $(1-P)/P$ was plotted as a function of $1/T$ and the resulting curves are shown in Fig. 4. In some cases the values of P close to 1.0 (or 100%) yield points which do not fall upon the best representative straight line. This indicates an inaccuracy in the assumed maximum value. In these cases, the correct value to make this point fall on the line was computed and the other values then recomputed.

As indicated in Fig. 4, the experimental points as predicted by the theory fall along straight lines within the experimental error in making the measurements. For example, it will be noted that the greatest deviations from the straight line occur at the lower end of the curves, i.e., at the higher values of efficiency. Here, an error of 1 or 2 per cent in determining P, or in setting its true maximum value, makes a very large difference in the value of $1-P$ and may result in large deviations. This condition is particularly noticeable in the case of the halophosphate and zinc-beryllium silicate where the efficiency remains high over a considerable range of temperatures. The equations of the lines in Fig. 3 are:

For magnesium tungstate $\log 1-P/P = -1850\ 1/T + 4.65$ (VII)

As shown in equation (V) the slopes of these curves give us measures of the activation energies of the radiationless states of the phosphors and the ratio of the maximum dissipation probability to the

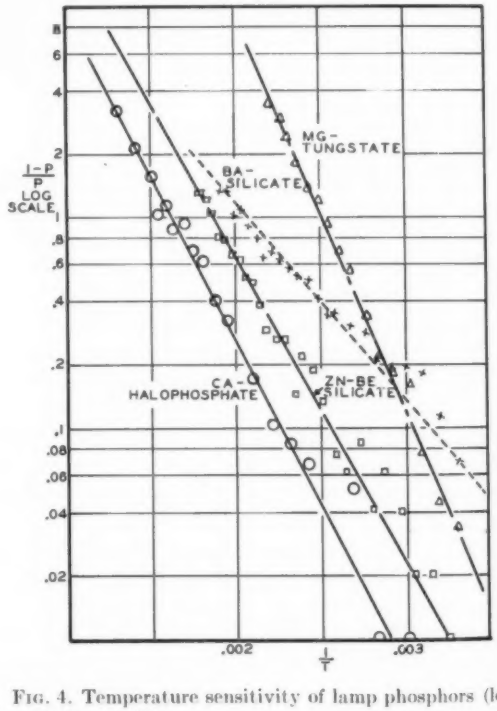

FIG. 4. Temperature sensitivity of lamp phosphors (log $(1-P)/P$ vs. $1/T$).

probability of the fluorescent process. These are listed in Table I. As pointed out earlier, the lamp data given in this table are probably in error due to the effect of the increased temperature on the operating characteristics of the lamp. They are presented here as being of academic interest and for comparison purposes.

There is very little information in the literature on activation energies of these phosphors. However, Kroeger and Hoogenstraaten (6) give values for

TABLE I. *Activation energies and probability of processes*

Phosphor	Plaque			Lamp		
	Activation energy (ϵ)			Activation energy (ϵ)		
	ergs $\times 10^{12}$	ϵv	B/A	ergs $\times 10^{12}$	ϵv	B/A
Magnesium tungstate	0.587	0.367	45,000	0.611	0.382	110,000
Zinc-beryllium silicate	0.456	0.285	496	0.403	0.252	417
Calcium halophosphate	0.492	0.308	356			
Mn band	0.456	0.285	182	0.108	0.068	1.38
Sb band	0.682	0.426	4,100	0.242	0.152	33.6
High Mn				0.166	0.104	5.25
Barium silicate	0.299	0.187	91			
Zinc orthosilicate				0.246	0.154	20.9

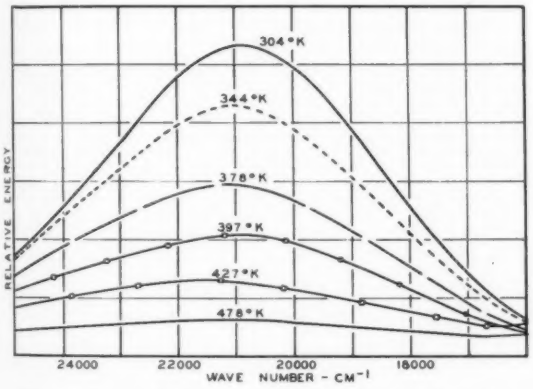

FIG. 5. Spectral energy distribution—magnesium tungstate.

zinc-beryllium silicates determined from decay rates which agree quite well with the value given by the above data.

EFFECT OF TEMPERATURE ON SPECTRAL ENERGY DISTRIBUTION

The effect of temperature on spectral energy distribution of phosphors in 40 T 12 lamps as described above was determined for magnesium tungstate (Fig. 5), zinc orthosilicate (Fig. 6), zinc-beryllium silicate (Fig. 7), and two calcium halophosphates: one with an appreciable antimony band (Fig. 8) and one with a high manganese content (Fig. 9) in which the antimony band is entirely suppressed.

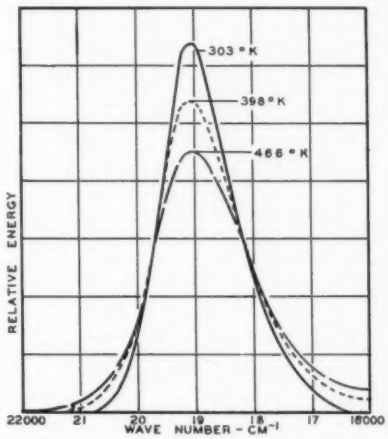

FIG. 6. Spectral energy distribution—zinc orthosilicate

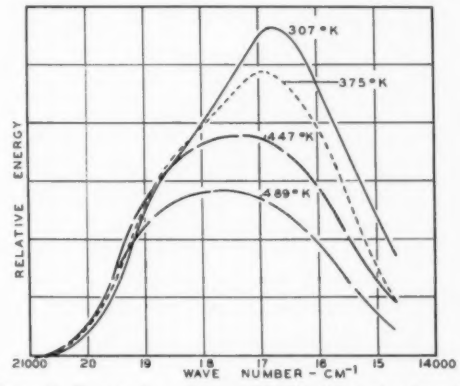

FIG. 7. Spectral energy distribution—zinc-beryllium silicate.

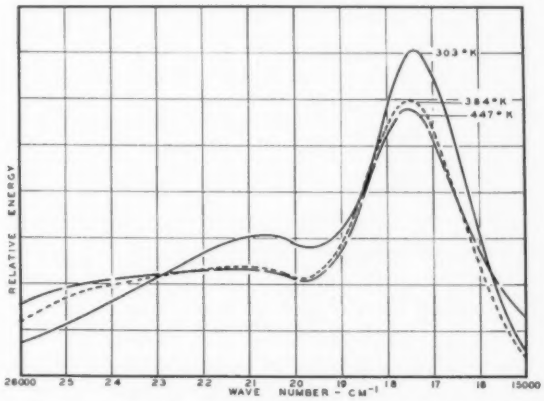

FIG. 8. Spectral energy distribution—calcium halophosphate.

The spectral energy distributions of these phosphors were resolved into their component Gaussian emission bands by the method described in a pre-

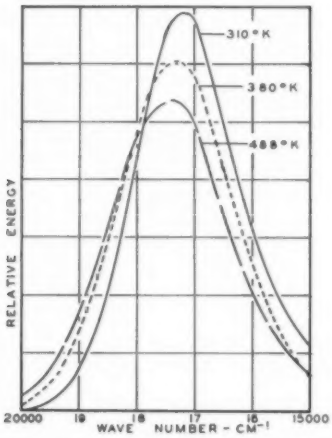

FIG. 9. Spectral energy distribution—high manganese halophosphate.

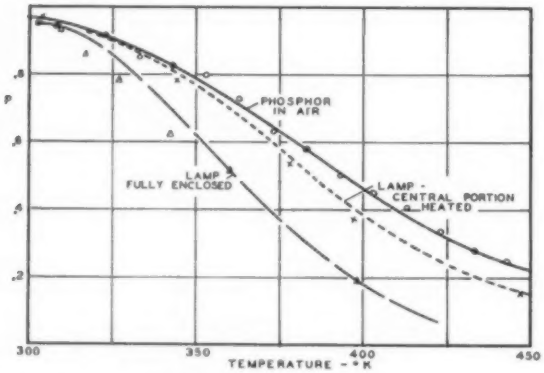

FIG. 10. Effect of temperature on magnesium tungstate

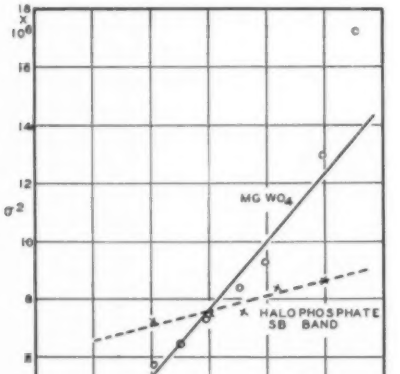

FIG. 11. Effect of temperature on emission band width (σ^2 vs. T).

vious paper (7). The testing of the two halophosphates was performed to check the accuracy in determining the Gaussian parameters of the manganese bands. Due to the method of analysis, procedural errors are cumulative and the precision falls off rapidly in the sequence of bands analyzed. Consequently, by choosing a halophosphate whose emission consists almost wholly of the manganese bands, a higher accuracy is obtained in the analyses of these emissions. However, the results indicate good agreement between the analysis of the manganese

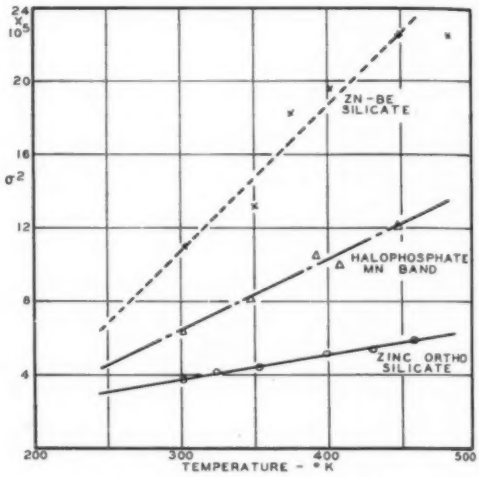

FIG. 12. Effect of temperature on emission band width (σ^2 vs. T).

TABLE II. *Gaussian analysis of magnesium tungstate emission*

Temp (°K)	$1/\lambda_0$(cm^{-1})	P	σ(cm^{-1})
304	20,750	0.950	2400
325	21,050	0.885	2540
344	21,200	0.770	2700
378	21,400	0.529	2900
397	21,375	0.370	3050
427	21,575	0.232	3350
447	21,700	0.159	3600
478	21,100	0.109	4150

bands from the phosphor with only manganese emission and that of the phosphor with considerable antimony emission. The relationship between σ^2 and T for the manganese band of halophosphate shown in Fig. 12 is the same for either case.

The results of the Gaussian emission analyses of these phosphors are tabulated in Tables II to VI. The maximum ordinate of the Gaussian band was taken as a measure of the intensity of the light and values of P computed therefrom as a basis of comparison for the results obtained with the plaques.

TABLE III. *Gaussian analysis of major emission band of zinc orthosilicate*

Temp (°K)	$1/\lambda_0$(cm^{-1})	P	σ(cm^{-1})
303	19,084	0.950	613
323	19,084	0.900	649
357	19,084	0.871	666
398	19,084	0.806	719
433	19,084	0.707	735
466	19,084	0.681	768

TABLE IV. *Gaussian analysis of emission of zinc beryllium silicate*

Temp (°K)	Major band			Minor band		
	$1/\lambda_0$(cm^{-1})	P	σ(cm^{-1})	$1/\lambda_0$(cm^{-1})	P	σ(cm^{-1})
307	16,700	0.970	1050	17,700	0.970	660
352	16,800	0.894	1150	18,750	0.80	690
375	16,950	0.826	1350	18,950	0.52	600
408	17,000	0.725	1400	18,950	0.48	650
447	17,100	0.641	1500	18,950	0.45	650
489	17,300	0.481	1500	19,150	0.36	600

TABLE V. *Gaussian analysis of major emission band of calcium halophosphate (high* Mn)

Temp (°K)	$1/\lambda_0$(cm^{-1})	P	σ(cm^{-1})
310	17,200	0.910	850
344	17,275	0.864	850
380	17,350	0.798	950
419	17,375	0.766	950
461	17,425	0.725	1075
488	17,450	0.705	1050

bands increase with rising temperatures and become an appreciable part of the over-all emission. Therefore, basing the emission solely on that of the major band could lead to spurious results.

Fonda (8) has found that the effect of a rise in temperature on phosphors containing two emission bands is to suppress the emission of the longer wavelength band and to enhance that of the shorter wavelength. This result is corroborated in the present study by the behavior of the antimony emission of the halophosphate. However, the manganese emission of this phosphor, which also consists of two bands, does not conform to this theory. In this case, both bands are initially suppressed with rising temperature with the minor band (longer wavelength) passing through a minimum and increasing again at high temperatures. Also, the analysis of the emission of zinc-beryllium silicate given in Table IV indicates that both bands decrease in intensity with rising temperature with the shorter wavelength band decreasing more rapidly than the longer wavelength band.

It has been suggested previously (7) that the relative intensities of multiple band emissions are determined by the atoms surrounding the activator. It seems logical to assume that the vibrations set up in the crystal lattice by increased temperatures may upset the balance determining the relative probabilities of the energy transfers. Consequently, a rise in temperature not only increases the probability of a radiationless transition, but also may vary the relative probabilities of the radiating transitions.

TABLE VI. *Gaussian analysis of calcium halophosphate emission*

Temp (°K)	Minor Sb			Major Sb			Major Mn			Minor Mn		
	$1/\lambda_0$(cm^{-1})	A	σ(cm^{-1})	$1/\lambda_0$(cm^{-1})	P	σ(cm^{-1})	$1/\lambda_0$(cm^{-1})	P	σ(cm^{-1})	$1/\lambda_0$(cm^{-1})	A	σ(cm^{-1})
303	25,500	3.0	1500	20,600	0.910	2700	17,300	0.910	800	15,750	9.0	525
346	25,400	5.0	1500	21,000	0.835	2700	17,300	0.877	900	15,500	8.0	600
384	25,300	8.5	1300	21,400	0.713	2750	17,350	0.828	1025	15,600	3.0	550
416	25,300	8.0	1350	21,500	0.667	2900	17,400	0.836	1000	15,400	7.5	725
447	25,650	9.4	1850	21,500	0.606	2940	17,350	0.812	1100	15,250	10.0	700

These values are listed in the tables as the maximum ordinate of the Gaussian band.

The plots of log $(1-P)/P$ against $1/T$ from the data in the above tables give straight lines which show good agreement in slope with those in Fig. 4, with the exception of the halophosphate. The latter phosphor gave a line with a much smaller negative slope than that obtained in the experiment of heating the phosphor in air. This is probably due to the emission in the lamp experiments being taken as proportional to the maximum ordinate of the main Gaussian emission band and ignoring the minor bands. As shown in Table VI and in Fig. 8 the minor

This effect, then, should depend on the composition of the lattice, and would not be expected to be the same for every type.

Except for the halophosphate, the plots of log $(1-P)/P$ against $1/T$ from the lamp experiments have essentially the same slope as their plaque counterparts, but are displaced slightly toward lower temperatures, the shift being of the order of magnitude of 20° at the higher temperatures. This is shown in the comparison curves of magnesium tungstate shown in Fig. 10. This is probably due to heat losses to the surrounding air in the plaque tests giving a slightly lower temperature to the phosphor than

that indicated by the thermocouple. The tests with the lamps, in which the whole area is enclosed, should give a closer agreement between the indicated and real temperatures.

TABLE VII. *Proportionality factors for σ vs. T* [equation (VI)] $\sigma = a(b + T)^{\frac{1}{2}}$

Phosphor	a	b
Magnesium tungstate	217	−187
Zinc orthosilicate	73	−18.6
Zinc beryllium silicate	88	−162
Calcium halophosphate		
Antimony band	105	+331
Manganese band	58	−112

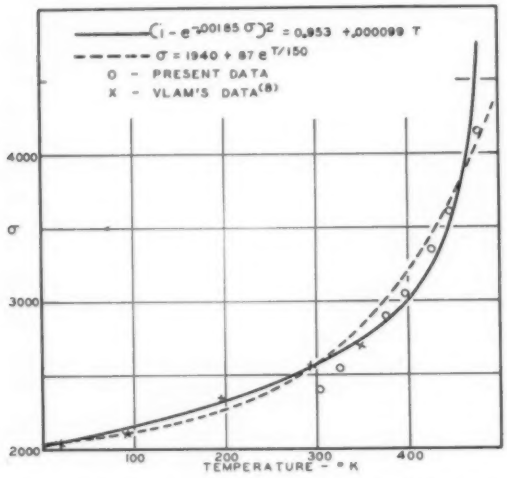

FIG. 13. Effect of temperature on band width of magnesium tungstate (σ vs. T).

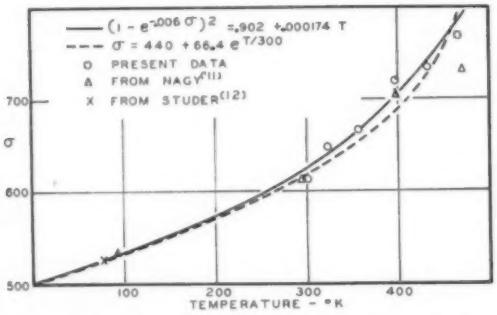

FIG. 14. Effect of temperature on band width of zinc orthosilicate (σ vs. T).

EFFECT OF TEMPERATURE ON BAND WIDTH

The theory advocated by Butler for the dependence of σ, or band width, on temperature predicts that σ^2 should be a straight line function of T [equation (VI)]. To test this relationship, σ^2 for the several phosphors was plotted against T as shown in Fig. 11 and 12. It will be noted that straight lines do give a good representation of these data. The values of the constants a and b of equation (VI) computed from these lines are tabulated in Table VII.

The value of b indicates the temperature at which the emission band should reduce to zero width—or become a spectral line. For example, magnesium tungstate should reduce to a line at 187°K. Of all the phosphors tested, the antimony band of the halophosphate is the only one which does not reduce to a line at some temperature short of absolute zero. Since it is known that none of these emission bands reduce to zero width at any attainable temperature, this result of these experiments is quite disturbing. Also, the work of Vlam (9) with magnesium tungstate gives values of σ down to 20°K which agree well with the present data where our ranges overlap, but do not fall along the same straight line.

The form of equation (VI) is derived from the assumption that the shape of the potential energy curve of an anharmonic oscillator is that of a parabola. This is true only very close to the equilibrium point.

Morse (10) gives a formula for the potential energy curve which holds throughout all amplitudes, of the form:

$$u = D[1 - \exp(-bX)]^2. \qquad \text{(XI)}$$

Starting with this equation, the relationship between σ and T becomes:

$$[1 - \exp(-a\sigma)]^2 = b + cT \qquad \text{(XII)}$$

The agreement of this formula with the observed data for magnesium tungstate is shown in Fig. 13. The values of the constants for the curve shown are:

$$a = 1.85 \cdot 10^{-3}$$
$$b = 0.953$$
$$c = 0.99 \cdot 10^{-4}$$

There is a dearth of data with which to check this formula for the other phosphors included in this study since band widths at very low temperatures are required. However, Nagy (11) and Studer and Gaus (12) give spectral energy distribution data for zinc orthosilicate at low temperatures from which the band widths could be computed. These data and those of the present study listed in Table III are shown plotted in Fig. 14. The curve shown is that computed from equation (XII) with the following constants:

$$a = 6.0 \cdot 10^{-3}$$
$$b = 0.902$$
$$c = 1.74 \cdot 10^{-4}$$

Fig. 13 and 14 show that reasonably good agreement with experimental data can be obtained by the use of this equation.

Due to the form of equation (XII), the constants must be determined by a trial and error method which can be quite tedious. There is another form for the equation of the interdependence of σ and T which, although purely empirical, fits the experimental points fully as well as the theoretically correct one. It is simpler and much easier to use. This equation takes the form:

$$\sigma = a + b \exp(cT). \qquad \text{(XIII)}$$

The agreement of this equation with the experimental data is shown in Fig. 13 and 14 as the dotted curve. The constants of this equation are:

For magnesium tungstate: $a = 1940$, $b = 87$, $c = 1/150$

For zinc orthosilicate: $a = 440$, $b = 66.4$, $c = 1/300$

From this study, it is concluded that simplified formulae for the interdependence of band width and temperature over a limited range of temperatures can be empirically derived. The form of these relationships is determined by the range of temperatures included. However, for a fully rigorous relationship equation (XII) must be used.

Acknowledgment

The author is particularly indebted to Dr. K. H. Butler for his many helpful discussions of the application of the data reported herein to the underlying theories.

Any discussion of this paper will appear in a Discussion Section, to be published in the June 1952 issue of the Journal.

REFERENCES

1. K. H. Butler, *J.* (*and Trans.*) *Electrochem. Soc.*, **95,** 267 (1949).
2. S. L. Parsons, A. E. Martin, and S. N. Roberto, *J. Electrochem. Soc.*, **97,** 41 (1950).
3. F. A. Kroeger, W. Hoogenstraaten, M. Bottema, and Th. P. J. Botden, *Physica*, **14,** 81 (1948).
4. N. F. Mott, *Proc. Roy. Soc.* (*London*) **A167**, 384 (1938).
5. F. Seitz, *Trans. Faraday Soc.*, **35,** 75 (1939).
6. F. A. Kroeger and W. Hoogenstraaten, *Physica*, **15,** 557 (1949).
7. K. H. Butler and C. W. Jerome, *J. Electrochem. Soc.*, **97,** 265 (1950).
8. G. R. Fonda, *J. Optical Soc. Am.*, **40,** 347 (1950).
9. C. C. Vlam, *Physica* **15,** 609 (1949).
10. P. M. Morse, *Phys. Rev.*, **34,** 57 (1929).
11. E. Nagy, *J. Optical Soc. Am.*, **39,** 42 (1949).
12. F. J. Studer and L. Gaus, "Effect of Temperature on the Spectral Energy Distributions of Several Phosphors," *Cornell Symposium on the Preparation and Characteristics of Solid Luminescent Materials*, John Wiley & Sons, Inc., New York (1948).

THE ELECTROCHEMICAL SOCIETY, INC.

The Electrochemical Society is an international organization of individuals and companies concerned with or interested in Electrochemistry and allied subjects.

The Society is dedicated to the advancement of the theory and practice of Electrochemistry and related subjects, as shown in the following divisions:

Battery	Electro-Organic
Corrosion	Electrothermic
Electric Insulation	Industrial Electrolytic
Electrodeposition	Theoretical Electrochemistry
Electronics	

Among the means to this end are the holding of meetings for the reading and discussion of professional and scientific papers on these subjects, the publication of such papers, discussions, and communications as may seem appropriate, and cooperation with chemical, electrical, and other scientific and technical societies.

It is an incorporated society without capital stock. The affairs of the Society are managed by a Board of Directors under a Constitution and By-Laws. Officers are nominated by a nominating committee appointed by the Board of Directors and elected by the members.

Direct all general correspondence and inquiries regarding membership to Society headquarters at 235 West 102nd Street, New York 25, N. Y., c/o Mr. W. J. Holian, Assistant Secretary.

Officers of the Society

President ..... Ralph M. Hunter
Past President ..... Charles L. Faust
Vice-President ..... J. C. Warner
Vice-President ..... Robert J. McKay
Vice-President ..... Marvin J. Udy
Treasurer ..... E. Gideon Widell
Secretary ..... Henry B. Linford